Chapter 1

General Introduction

GRAPHICAL ABSTRACT

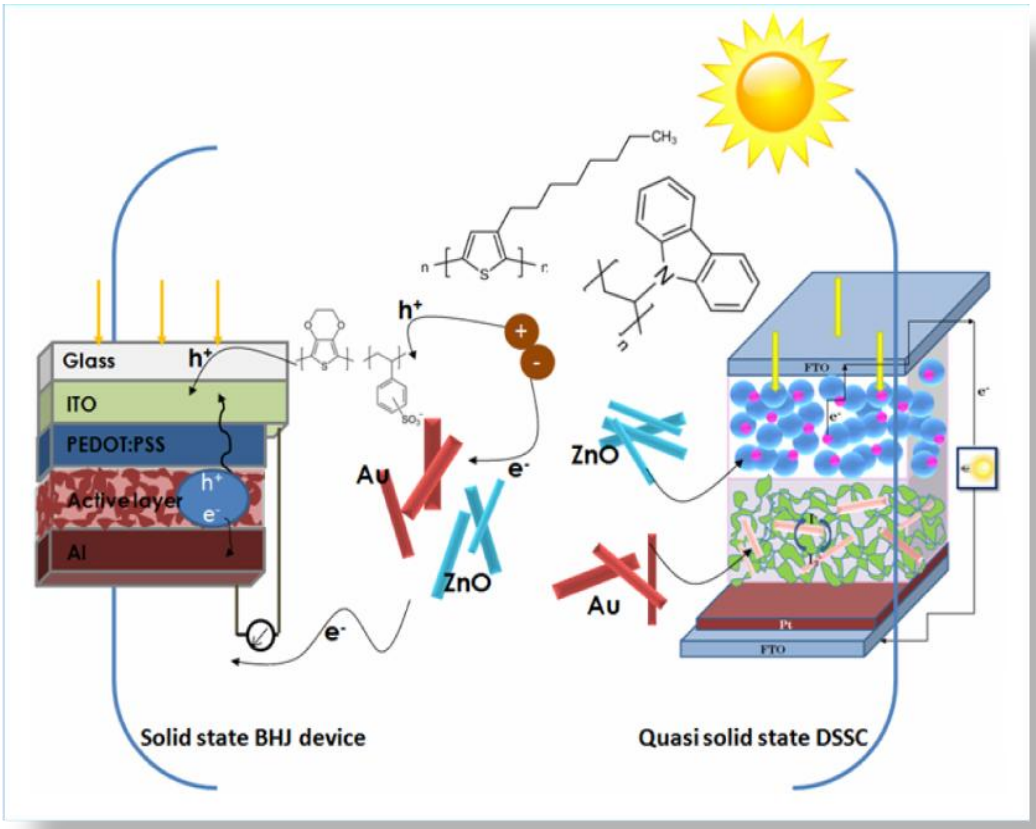

The chapter deals with motivation and research background of the present investigation with brief literature review on different materials and methods used in solar cell.

Dream is not that which you see while sleeping.....it is something that doesn't let you sleep.....

A.P.J. Abdul Kalam
(Former President of India)

1.1 Motivation and research background

With the rapid explosion of population in world, its energy demand has also reached the highest extent. It is expected that the world's power consumption will reach about 23 terawatts in 2050.[1] The fossil fuels meet 80% of the energy requirement of the whole world.[2] However, the burning of such fuels raises the amount of carbon dioxide in the atmosphere which offers threat to the environment. The energy sources like petroleum, coal and natural gas are causing serious damage to the environment and living organisms by emitting toxic and climate changing by-products. In recent scenario, the use of clean and renewable energy resources become very important for sustainability of the universe. There are many forms of renewable energy namely, wind energy, hydroelectric energy, biomass energy, geothermal energy, tidal energy and solar energy. Among these energy resources, solar radiation is one of the most promising and efficient energy that is abundant in nature. To our privilege, India is found to be rich in solar energy resources. The average intensity of solar radiation received on India is 200 MW/square km. With a total geographical area of 3.287 million square km, if only 10% of this area can be used for solar energy installations, the available solar energy would be 8 million MW which is equivalent to 5 909 million tons of oil per year.[3]

Solar radiation conversion systems can be categorized in three different classes:

- *Solar electricity*: conversion of solar radiation into electricity, viz., solar photovoltaics,
- *Solar fuels*: conversion of solar energy into chemical fuels, viz., artificial photosynthesis and
- *Solar thermal systems*: conversion of sunlight into storable, dispatchable thermal energy, viz., solar heating, solar architecture etc.

Photovoltaics', i.e., converting sunlight into electrical energy is a fast growing technology that can solely meet the world's growing energy demand without providing any threat to the environment. A solar cell or photovoltaic cell is an electrical device

that converts the energy of sunlight directly into electricity by the photovoltaic effect. It is a form of photoelectric cell, whose electrical characteristics, such as current, voltage or resistance vary when exposed to light. In 1839, Edmond Becquerel found that some materials in an electrolytic cell produced an electrical current under exposure to sunlight which he referred as the "photovoltaic effect".[4, 5] However, the first silicon solar cell was practically demonstrated by Daryl Chapin and his co-workers at Bell Laboratories in 1954.[6] So far various modified structures have been developed for inorganic solar cells that includes monocrystalline silicon, polycrystalline silicon, thin film (based on cadmium telluride (CdTe), copper indium gallium selenide (CIGS) and amorphous silicon (a-Si)) etc. Currently, these solar cells dominate the photovoltaic industry with efficiency of around 15-30%. However, due to the high cost and related environmental issues, the application of such inorganic solar cells have been partially impeded which paves the way to a less costly and environmentally benign alternative.

Organic-inorganic hybrid solar cells are one of the most promising alternatives to inorganic solar cells that require less production cost and produce flexible devices. Polymers are used to fabricate different solar cell architectures. Among all these, bulk heterojunction (BHJ) and dye sensitized solar cells (DSSCs) are the most important in terms of stability and efficiency. In a polymer based hybrid BHJ cell, a long-chained molecular system e.g., poly(3-hexylthiophene) (P3HT), Poly[2-methoxy-5-(3′,7′-dimethyloctyloxy)-1,4-phenylenevinylene] (MDMO-PPV) is used as the electron donor and a fullerene derivative e.g., Phenyl-C_{60}-butyric-acid-methyl ester ($PC_{60}BM$), Phenyl-C_{70}-butyric-acid-methyl ester ($PC_{70}BM$) as the electron acceptor. Polymer based hybrid solar cell is most efficient because of the following facts:[7]

- Polymer based solar cells can form very thin films (1000 times thinner than silicon cells) due to the molecular nature of the materials. So, requires less fabrication cost.
- The polymer synthesis methods (viz., solution process, roll-to-roll technology) require low energy and temperature compared to their conventional counterparts.
- Various molecular properties (viz., band gap, molar mass etc.) can be tuned by modifying the length and functional groups of the polymer and also by

incorporating various nanofillers into the polymer matrix.

- These are amazingly lighter and flexible as compared to their rigid counterparts and that is why, easy to storage and transport, less prone to damage and failure.

One of the most important photovoltaic (PV) technologies is the DSSCs which are considered as a third-generation PV device. The devices are important due to their low-cost and environmentally-friendly fabrication process. Polymers may play different roles in a DSSC. Depending on their versatility in properties, polymers can replace the liquid electrolytes or the counter electrode.

In the present thesis, we are trying to emphasize on the improvement in BHJ and DSSCs.

1.2 Bulk heterojunction (BHJ) solar cells

Organic semiconductors such as conjugated polymers have attracted a great deal of attention in recent times which was first put forward with the BHJ concept. The active layer of a BHJ consists of a nanoscale blend of donor and acceptor materials which more or less eliminates the drawbacks related to planer bilayer heterojunction. The working principle of a BHJ solar cell can be summarized as follows:

- Absorption of sunlight by the active layer and generation of highly localized, tightly bound Frenkel excitons. An exciton is defined as the electron-hole pair bound by strong coulomb interaction.
- Exciton diffusion to the donor-acceptor interface,
- Exciton dissociation at the interface creating charge transfer (CT) states or so-called polaron pairs, followed by dissociation of the CT states into free charge carriers,
- Charge transport and collection by the respective electrodes.

Due to the large donor acceptor interfacial area, the exciton dissociates into electron and hole and transport to the respective electrodes. Electrodes with different work functions are required for effective exciton dissociation. Otherwise, the diffusion will act as a driving force on the free charge carriers thus promoting their recombination.[8] The difference in work function between two electrodes in a BHJ cell creates a

potential in the interface which can facilitate the dissociation of exciton and transport of charges towards the respective electrodes. However, for an efficient BHJ the domain size should be large enough so that it can form a percolating network for the transport of charges. Without this network charge separation is not possible as the charges might be trapped in donor or acceptor rich domain and recombine. Usually the two components of the BHJ solar cell are a conjugated polymer based donor and fullerene or other nanoparticle based acceptor. The two components in the device self-assemble into an interpenetrating network that connects the two electrodes.

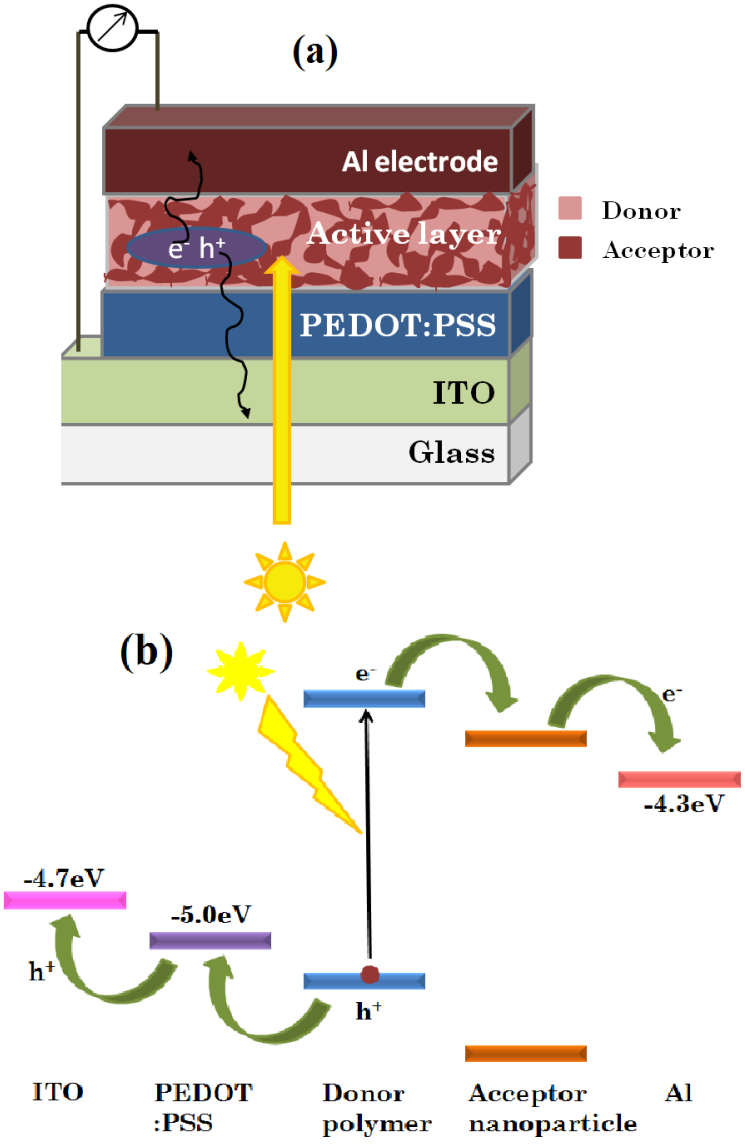

Fig. 1.1 (a) Schematic representation of a BHJ device, (b) Working principle of a BHJ device.

In 1839, the concept of PV effect arises after the discovery of a photocurrent generated in a photoelectric cell under exposure to sunlight.[4, 5] In the beginning of the 20th

century, photoconductivity was first observed on anthracene. Tang reported in 1986 the first successful organic photovoltaic device for p-type copper phthalocyanine and n-type bis-benzimidazo[2,1-a:2′,1′-a]anthra[2,1,9-def:6,5,10-d′e′f′] diisoquinoline-10,21-dione.[9] A photo conversion efficiency (PCE) of about 1% with a high fill factor (FF) of 65% was observed for a bi-layer configuration of the device. After six years, Heeger and Wudl groups individually developed the donor acceptor PV devices by using a conjugated polymer, poly[2-methoxy-5-(2-ethylhexyloxy)]-1,4-phenylenevinylene (MEH-PPV) as the electron donor and fullerene (C_{60}) derivatives as electron acceptors.[10, 11] In the contemporary period, the concept of BHJ arises which introduces the idea of the limited exciton diffusion length in organic solar cells.[12, 13] This was a serious fault for previous organic solar cells. BHJ structure based on polymer/fullerene blend was introduced in 1995 by Heeger and his co-workers by using MEH-PPV as the donor and $PC_{60}BM$ as the acceptor in the active layer.[13] Concurrently, Friend and his group demonstrated the BHJ structure for all polymer blends where both the donor and acceptor roles are played by different polymers.[12] Further studies showed that the domain sizes of donor and acceptor can be optimized with additives.[14, 15] It is found that the BHJ morphology can be controlled by introducing various additives into the donor-acceptor mixture. A class of 1,8-di(R)octanes with I or Br functional groups (R) as processing additives shows the best results. Moreover, studies show that by introducing substituents on the polymer backbone the energy levels of the polymer can be modified.[16] In the context of hybrid photovoltaics, the most employed organic electron acceptor material is fullerene and its derivatives, due to its very high electron affinity and strong charge transport ability. But the high photon-to-electron conversion yield needs an interpenetrating and percolating network comprising of both donor and acceptor molecules within the exciton diffusion length of the donor polymer, typically of the order of a few tens of nanometres. In this frame of reference, the emergence of inorganic nanocrystals has suddenly revealed the concept of hybrid BHJ devices. In such devices the organic acceptor material is substituted by the inorganic nanocrystals.

The hybrid BHJ structure consists of both organic polymer and inorganic nanostructures in the active layer. Organic conjugated polymers serve as the donor that absorbs light and transport holes and the inorganic materials serve as the electron

acceptor. Furthermore, such organic-inorganic hybrid devices offer several attributes. These are morphologically more stable, flexible and solution processable in addition to their high charge carrier mobility.[17, 18] Nanocrystalline inorganic semiconductors have numerous advantages as an electron acceptor such as high electron mobility and electron affinity, significant chemical and physical stability etc. Recently, one-dimensional nanostructures (viz., nanorods, nanotubes etc.) attain preferable utilization in solar cells as the structures are potential for providing a continuous and one-dimensional path for charge transport. This reduces charge recombination inside the active layer.[19, 20] Furthermore, the feasibility of the synthesis of nanorods in solution phase at low temperature (<300 °C) and the re-dispersion at different solvents provide low-cost techniques for the fabrication of large area devices.[21]

1.2.1 Nanoparticles of interest

Zinc oxide (ZnO)

During last few decades, the use of semiconductor metal oxide nanocrystals, especially titanium dioxide (TiO_2) and ZnO in hybrid BHJ devices have shown a lot of interest. ZnO nanocrystals have manifold applications in the field of solar photovoltaics,[22, 23] short wavelength optoelectronic devices[24, 25] and sensors[26] as they possess unique properties. Such properties include wide band gap, large exciton binding energy[27, 28] high carrier mobility, ease of fabrication, non-toxicity and relatively low production costs. Hybrid BHJ solar cells employing vertically oriented ZnO nanorod arrays were first exploited by various groups [22, 29, 30] with a maximum PCE of 0.53%. A simple method is employed to fabricate a hybrid BHJ device by using porous ZnO and P3HT. Spin coating of ZnO nanocrystals onto indium tin oxide (ITO)/dense ZnO film and followed by sintering into a nanoporous ZnO layer leads to the fabrication of a hybrid P3HT/ZnO solar cell with a maximum PCE of 0.35% for 8x13 nm ZnO nanorods.[31] The PCE of 1.6% is achieved for blends of MDMO:PPV/ZnO[32, 33] which is four-fold greater than conjugated polymer/TiO_2 blend based hybrid BHJ devices.[34, 35]

Further studies investigate the effect of various parameters, including concentration of ZnO, ligand exchange and nanoparticle size and shape on device performance.[33, 36] 4.9 nm diameter nanocrystals show the maximum efficiency. Hybrid BHJ photovoltaic

device with PCE of 1.23% and a fill factor (FF) of 47% is made from vertically aligned ZnO nanorods.[37] Recently, a hybrid BHJ solar cell composed of Poly(3-hexylthiophene) (P3HT)/ZnO combined with 650 nm long ZnO nanorod arrays has been fabricated with a PCE of 0.45%.[38] In polymer/ZnO nanoparticle blend structure, the surfactant of the nanoparticle affects adversely on efficiency, although it is required for better dispersibility.

Table 1.1 Summary of photovoltaic parameters for the polymer/ZnO approaches based on BHJ geometries

	J_{sc} $mAcm^{-2}$	V_{oc} V	FF %	η %	Irradiance ($mW\ cm^{-2}$)	Ref
Nanostructured metal oxide/polymer approaches						
ITO/ZnO fibers/P3HT/Ag	2.17	0.44	56	0.53	100	[29]
ITO/NR-ZnO array/Z907/P3HT/PEDOT:PSS/Au	1.73	0.30	39	0.20	100	[41]
ITO/NS-ZnO/P3HT/Au	2.18	0.36	44	0.35	100	[31]
Nanocrystal/polymer blends						
ITO/PEDOT:PSS/NC-ZnO:MDMO-PPV/Al	2.40	0.81	59	1.60	71	[32]
ITO/PEDOT:PSS/NC-ZnO:P3HT/Al	2.19	0.69	55	0.92	75	[42]
ITO/PEDOT-PSS/P3HT:ZnO/Li/Al	3.50	0.83	50	1.4	50	[39]
ITO/PEDOT:PSS/ZnO:P3HT/Al	5.20	0.75	52	2.0	50	[40]
ITO/PEDOT:PSS/ZnO:P3HT-E/Al	2.10	1.02	40	0.83	50	[43]
ITO/NC-ZnO/NC-ZnO:P3CT/PEDOT-PSS/Ag	1.00	0.52	35	0.18	100	[44]

*J_{sc}-photocurrent density, V_{oc}-open circuit voltage, FF-fill factor, NR-nanorod, NS-nanosphere, NC-nanocrystal, PEDOT:PSS- poly(3,4-ethylenedioxythiophene) polystyrene sulfonate, P3CT-poly(3-carboxydithiophene)

This may be due to the presence of energetic barriers between the nanoparticles. In order to overcome the challenges, in-situ synthesis of polymer nanocomposites attracts a large number of researchers in recent times.[39, 40] The best hybrid BHJ solar cell is obtained with an active layer thickness of 225 nm and PCE of 2%.

Gold (Au) plasmonic nanoparticle

In a typical hybrid BHJ photovoltaic device, the optimum thickness of the active layer of the order of 100-200 nm which can offer very low absorption of light. Therefore, thickness of the film should be greater for efficient light absorption. However, the thicker layer may be detrimental to efficiency enhancement as it increases the device resistance due to low carrier mobility and short exciton diffusion length.[45] So, we need a material that can cause light trapping inside the active layer. It can enhance the light absorption without increasing the thickness. In the light of this issue, plasmonic nanostructures play a crucial role. Recently, plasmonic becomes one of the most extensively studied topics of research since 2000. The "plasmonic" describes mainly the interaction between electromagnetic radiation and conduction electrons at the metal/dielectric interface. The metallic nanoparticles generally show a quantized excitation arises in the presence of conduction electrons. This quantized excitation is known as the surface plasmons.[46] The surface bound electromagnetic waves, i.e., the surface plasmons are coupled to electron density oscillations and thus confined to the metal nanoparticle interface well below the diffusion limit, λ_0/n (where, 'λ_0' is the wavelength in vacuum and 'n' is the refractive index of the surrounding environment). This can overcome the size incompatibility felt between optical devices and current micro-fabrication techniques. All the illuminated particles are excited and strongly absorb or scatter the incident light thus creating the localized surface plasmon resonance (LSPR). The surface plasmon resonance (SPR) of metallic nanoparticles mostly occurs in the visible and near infra-red region. Therefore, the incorporation of these nanoparticles into a hybrid BHJ device can enhance the total light absorption inside the BHJ. A plasmonic nanostructure as an efficient light scattering and trapping agent can reduce the physical thickness of present solar cells, at the same time maintain the optical thickness.[46] When a plasmonic metal nanoparticle is incorporated into a photovoltaic device, the high electromagnetic field strength in the

neighbourhood of the excited surface plasmons causes improved light absorption. Consequently, the J_{sc} as well as the overall conversion efficiency can be enhanced.[47]

Anisotropic metallic nanoparticles are superior light absorber over spherical ones in the sense that the LSPR varies with the shape of the nanoparticle. Depending on various orientations of the particle axes two or more resonance modes appear. For instance, a symmetrical particle, i.e., a nanosphere shows only one dipolar plasmon resonance, but in case of one-dimensional nanoparticles, such as nanorods an additional dipolar resonance band appears in the longitudinal direction known as the longitudinal mode of vibration. Similarly, for nanoparticles with more complex geometry, multiple resonance modes appear. A highly symmetric spherical nanoparticle exhibits a single scattering peak, while anisotropic shapes exhibit multiple scattering peaks in the visible wavelengths due to highly localized charge polarizations at corners and edges. Thus, the optical properties can be improved. For anisotropic nanoparticles, the higher multipolar SPRs are always situated at the longer wavelengths with respect to the dipolar ones (red-shifted).[48] Therefore, with increase in anisotropy, the optical absorption shifts towards visible range which is the main condition for an absorber material in BHJ solar cells. Although numerous metal nanoparticles are receiving research interest, the most studied particle of interest is Au due to its photostability in air environment, large scattering cross section and rich chemistry for the surface functionalization.[49]

The plasmonic enhancement in light sensitive devices was pioneered by Stuart and Hall.[50] It was observed that the resonance associated with metal island films could be used in sensitivity enhancement of very thin semiconductor photo-detectors. It is also found that the cylindrical and hemispherical nanoparticles increase the path length more as compared to spherical nanoparticles due to the enhanced near-field coupling. Previous studies showed that the incorporation of metal nanoparticles enhances optical absorption and offers enhanced carrier mobility as the conductivity of such nanoparticles is more than organic molecules.[51] Wang et al. have investigated the photovoltaic property of organic solar cells using Au nanoparticles into a newly synthesized donor polymer poly[2,7-(9,9-dioctylfluorene)-alt-2-((4-(diphenylamino)phenyl) thiophen-2-yl) malononitrile] (PFSDCN). It was found that

increased concentration of Au nanoparticles upto an optimum level facilitates the improvement of the optical absorption due to LSPR effect of Au nanoparticles.[51] Above this optimum concentration, there is an adverse effect. A very high concentration forms a nanoparticle-induced morphology that makes it difficult to extract carriers before undergoing recombination and consequently reduces the cell performance.

Kim and Carroll, for the first time reported the incorporation of small amounts of Au and Ag metal nanoparticles into the photoactive layer.[52] The insertion of dopant states into the active layer or the interface enhances the electrical conductivity thus reducing the series resistance. As a consequence of this, device performance is enhanced by 70%. However, the improved light absorption due to scattering has a minor effect in this regard. The surfactant free laser ablated Au nanoparticle insertion into the active layer leads to increased PCE by 40% which is studied by Stylianakis group. The improvement is caused by the enhanced light harvesting in the BHJ due to localized SPR and scattering effect of nanoparticles.[53] In presence of 70 nm truncated octahedral Au nanoparticles into the poly[N-9˝-hepta-decanyl-2,7-carbazole-alt-5,5-(4′,7′-di-2thienyl-2′,1′,3′-benzothiadiazole (PCDTBT):$PC_{70}BM$ photoactive layer, the PCE of a BHJ device is enhanced by 13% from 5.77% to 6.45% which is due to the improved scattering from the large truncated structures.[54] When Au nanoparticles are embedded into the hole-transporting layer (HTL) PEDOT:PSS, it is demonstrated to be effective in enhancing the performance due to large hole collection and reduced exciton quenching.[55] In this case, Au nanoparticles offer only a minor contribution towards the optical absorption. Rather, a minute amount of nanoparticle provides significant contribution in reduction of resistance inside the HTL.

The first report on photovoltaic performance of Au nanoparticles embedded into the PEDOT:PSS (HTL) was provided by Chen et al.[56] The exciton dissociation rate and the probability of exciton dissociation is enhanced with the insertion of nanoparticles with subsequent increase in J_{sc} and FF. Blend of PEDOT:PSS with Au nanospeheres and nanorods of various sizes and shapes improves the efficiency by 24% due to the combined effect of both LSPR and scattering.[57] When ultrafast and laser-ablated Au and Ag nanoparticles were placed at the interface between PEDOT:PSS and the

photoactive layer, a 20% enhancement in PCE was observed. This is because of the enhancement of J_{sc} in the device due to LSPR of the nanoparticles.[58] By applying a layer-by-layer electrostatic assembly, Au nanorods were deposited onto the ITO film followed by transformation of these nanorods into nanodots through a thermally induced shape transition. A PCE of 3.65% is observed which is attributed to the presence of the plasmon field in the surrounding of the nanodots.[59] Placement of 7-9 nm Au nanowire network, based on solution-phase synthesis at the ITO/PEDOT:PSS interface acts as the plasmonic antennae and offer PCE of 2.72% due to the scattering effect.[60]

Table 1.2 Device characteristics of hybrid photovoltaic devices with Au nanoparticles embedded in various configurations

Nanoparticle	Photoactive layer	η (%)	Mechanism	Ref
Nanoparticles dispersed into the active layer				
70 nm nanoparticles	PCDTBT:$PC_{70}BM$	6.45	Scattering	[54]
4.8-7.4 nm nanoparticles	POT-C_{60}	1.9	Electrical	[52]
10 nm nanoparticles	P3HT:PCBM	3.71	LSPR and scattering	[53]
Nanoparticles dispersed into the HTL (PEDOT:PSS)				
30-40 nm nanoparticles	P3HT:PCBM	4.19	LSPR	[56]
3 nm nanoparticle and 12 nm nanorods	P3HT:$PC_{60}BM$	4.28	LSPR and scattering	[57]
18 nm nanoparticles	P3HT:PCBM	3.51	Electrical	[55]
Nanoparticles dispersed between interfacing layers				
30 nm nanodots at the ITO/PEDOT:PSS interface	P3HT:PCBM	3.65	Plasmon	[59]
20 nm Au and Ag nanoparticles	P3HT:PCBM	1.5-2.4	LSPR	[58]
7-9 nm nanowires at the ITO/PEDOT:PSS interface	P3HT:PCBM	2.72	Far field scattering	[60]

1.2.2 Polymers used in solar cell

Poly(3-alkylthiophene) (P3AT)

Although people were focussing their research on poly(p-phenylene vinylene) (PPV)-based polymers for hybrid BHJ solar cells, still the large band gap (>2eV) of the polymer and low photocurrent impeded further optimization. Therefore, in simultaneous period research interest shifted to polythiophene and its derivatives.[61, 62] The band gap of such polymers is <2eV and with increasing the quinoidal character in the polymer further band gap reduction may be achieved.[63] In general, P3AT solar cells offer high external quantum efficiency (EQE) of ~88%. Moreover, by modifying various parameters like applying thermal or vapour annealing, increasing regioregularity etc., PCE of >5% can be achieved.[64, 65] In case of conjugated polymers, the side chain plays an important role. It offers improved solubility and processibility of the polymer by reducing π–π inter-chain interaction and determines the intermolecular interactions between different polymer chains. You et al. investigated the effect of size and position of side-chain on the photovoltaic performance of conjugated polymers. The PCE of the polymer: [6,6]-phenyl-C_{61}-butyric-acid-methyl ester (PCBM) device increases from 0.7% for polybenzo[2,1-b:3,4-b′]dithiophene-4,7-Di(thiophen-2-yl)benzothiadiazole (PBDT-DTBT) to 2.2% for PBDT-4DTBT.[66] In 2010, Zhao et al. developed a BHJ solar cell using (P3HT):indene-C_{60} bisadduct (ICBA) as the active layer. After thermal annealing, a remarkably high PCE of 6.5% was achieved with an impressive V_{oc} value of 0.84V. The higher value of device parameters is attributed to the increased energy in lowest unoccupied molecular orbital (LUMO) of 0.2 eV for ICBA than PCBM.[65] The same group observed better PCE of 7.4% for the same active material with optimization of device conditions.[67]

Lee et al. provided a simple oxidative polymerization method to the formation of poly(3-octylthiophene) (POT)/double walled carbon nanotubes (DWCNTs). It is revealed that the DWCNTs are unique in their multiple properties. The inner tube retains its intrinsic electronic and optical properties, while the outer tube could be involved in the composite formation. The nanohybrid material with effective interface offers an exciting Hall mobility of 2.193×10^{2} $cm^2/V.s$ with a carrier concentration of 7.228×10^{14} cm^{-3}. It makes them efficient as a photoactive material.[68]

By applying some specific fabrication conditions and post-production annealing

treatment at 150 °C, Heeger and group demonstrated a PCE of 5% using P3HT/PCBM as the active layer.[64] A new class of low band gap co-polymers, poly[2,6-(4,4-bis-(2-ethylhexyl)-4H-cyclopenta-[2,1-b;3,4-b′]-dithiophene)-alt-4,7-(2,1,3-benzothiadiazole)] (PCPDTBT) was investigated where a cyclopenta-di-thiophene unit acts as the donor block in the polymer chain. By blending with PCBM, the co-polymer shows PCE of 3.2%, J_{sc} of 10-11 $mAcm^{-2}$ and a reasonably high EQE of more than 25% over the spectral range from 400 to 800 nm. PCPDTBT is the first low band gap conjugated polymer with highly efficient photovoltaic activity in the IR spectral region.[69] In 2008, M. Lenes et al. demonstrated a novel fullerene derivative, bisadduct analogue of PCBM (bis-PCBM) in a series of BHJ solar cells with a higher LUMO level compared to PCBM. This minimizes the energy loss during electron transfer from the donor (P3HT) to the acceptor. The higher LUMO results in a significantly enhanced V_{oc} and PCE of 0.73 V and 4.5% respectively for a P3HT:bis-PCBM solar cell.[70]

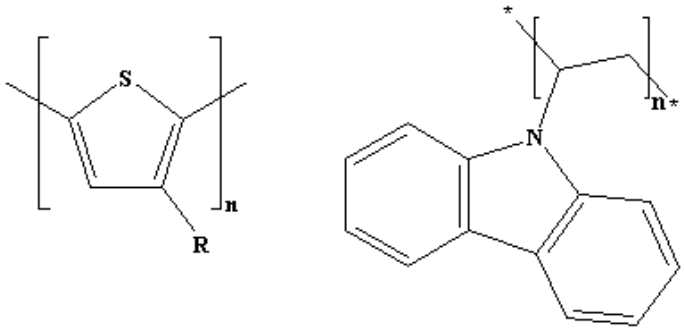

Fig. 1.2 Chemical structure of Poly(3-alkylthiophene) and Poly(9-vinylcarbazole)

Poly(9-vinylcarbazole) (PVK)

Followed by the PPV, P3AT and their derivatives, the most studied conjugated polymer in BHJ devices is the PVK. In 1958, Hoegel et al. for the first time proposed the practical application of PVK as a photographic agent.[71] Carbazole-based polymers have numerous advantages as a photoconducting and charge transporting material:[72]

- carbazole is a low-cost material which can be readily achieved from coal-tar distillation,
- carbazole group can easily form relatively stable radical cations, i.e., holes,
- part of carbazole containing compounds offer relatively high charge carrier

mobilities,

- it is easy to introduce different substituents into the carbazole ring and
- carbazole containing compounds are highly thermally and photochemically stable.

G. Wang et al. studied the usefulness of multilayer PVK/C_{60} film in controlling the charge transfer process in a set of organic solar cells.[72] The physical jet deposition technique was used to fabricate the PVK/C_{60} film, where PVK and C_{60} molecules are combined at the molecular level. This gives rise to a remarkable enhancement of photovoltaic signal by five orders than their pristine polymer. This enhancement is due to the efficient charge separation at the PVK/C_{60} interface thus offering a very fast electron transfer inside the cell. The insertion of TiO_2 nanoparticles into PVK matrix shows that a significant photo-response in terms of J_{sc} and FF can be achieved by controlling the interfacial area between donor and acceptor and an optimum concentration of TiO_2 nanoparticle dispersed into the polymer matrix.[73] Layered PVK/TiO_2 nanocomposite films are prepared by a spin-coating method. It is observed that the nanocomposite film absorbs light mainly in the ultraviolet (UV) region which makes them efficient candidate for UV photovoltaic devices.[74] The synthesis of three-armed and uniform cadmium sulfide (CdS) nanorods followed by the formation of a nanocomposite material with PVK is carried out. The synthesized nanocomposite shows a remarkable decrease in photoluminescence (PL) efficiency simultaneously providing an enhanced photovoltaic signal. The energy level matching between the donor and acceptor facilitates fast exciton dissociation inside the active layer and interfacial charge transfer.[75] The photovoltaic properties of N-alkyl substituted polycarbazole derivatives such as poly(9-dodecylcarbazole) (PDDC) and poly[(9-dodecylcarbazole)-co-thiophene] (PDDCT) are studied by blending the polymer with TiO_2. It is observed that the PCE of the devices increases from 0.11% to 0.18% for PDDC and from 0.14% to 0.24% for PDDCT upon annealing at 150 °C for 30 min. This enhancement is due to the spatial rearrangements of the polymer chains. This leads to tight stacking and a strong inter-chain interaction thereby increasing the light absorption ability. Moreover, PDDCT-based device exhibits relatively better PCE than PDDC-based device due to the higher donor ability of PDDCT than PDDC.[76]

1.3 Dye sensitized solar cells (DSSCs)

The second main strategy in the development of polymer based hybrid photovoltaics arises with the concept of DSSCs. The importance of such device may be realized as they show comparatively high PCE, cost-effective fabrication process, environmental friendliness etc.[77] A DSSC is a class of solar cell belonging to the thin film solar cells. A DSSC is mainly composed of a photosensitized or dye sensitized anode comprising a semiconductor oxide, a photoelectrochemical system, i.e. an electrolyte and a metal counter electrode. The charge generation and transport mechanism in such architecture is somewhat different from the donor-acceptor BHJ device. The charge generation occurs at the semiconductor-dye interface, while the charge transport is carried out by the semiconductor and the electrolyte. By optimizing semiconductor and electrolyte composition the charge transport properties can be tailored, while for spectral property optimization the modification of dye composition is only necessary.[78] The operational principle in a DSSC can be explained as:[79]

- The photoexcitation of the photo-sensitized dye molecule adsorbed on metal oxide semiconductor from the ground state (D) to the excited state (D*) after illumination of sunlight, followed by emission of photogenerated electrons,
- Injection of photogenerated electrons of dye molecule into the mesoporous semiconductor metal oxide networks filled with a liquid redox electrolyte,
- Rapid transfer of electrons to the conduction band (CB) of the semiconductor interfaces,
- Location of the electrons in the CB and the holes left in the oxidized dye resulting in the separation of charge carriers,
- Transportation of the injected electrons in the CB across the metal oxide film by diffusion towards fluorine doped tin oxide (FTO) substrate and then to the external circuit generating a flow of current. This process is ultrafast and initiates conversion of light into electricity in the DSSC.
- Regeneration of the oxidized dye to its neutral state by receiving ground-state electrons from redox mediators, (usually comprised of iodide/triiodide (I^-/I_3^-)) in the electrolyte and transportation of the positive charges to electrically connected counter electrode.

We refer the DSSC as the hybrid photovoltaic device because of the use of polymer based electrolytes in these devices. The conventional liquid electrolyte based DSSC has been suffering from some important drawbacks. Such difficulty arises regarding their long-term stability due to the challenges in integration of large area modules, in sealing issues, possible desorption, photodegradation of the attached dyes with the liquid electrolyte and corrosion of the counter electrode.[80] Therefore, in order to counteract this durability issue, gel polymer based electrolytes are being investigated that can substitute the liquid electrolyte.[77, 81]

1.3.1 Polymer electrolyte based solar cells

According to Fenton, polymer materials are generally complexed with a salt to form the polymer electrolyte.[82] Polymer chains consist of polar functional groups that solvate the ionic species of the salt by intermolecular interactions. These ions are transported through the free volume of the polymer marix. Fenton et al. found a high ionic conductivity of 10^{-5} Scm^{-1} when poly(ethylene oxide) (PEO) is complexed with sodium thiocyanate (NaSCN) salt.[82] The discovery reveals the use of solid-state electrochemical devices for energy storage. Since then a number of research activities have been carried out on various types of polymer electrolytes.

Polymer electrolytes generally include solid-state polymer electrolytes, gel based polymer electrolytes and hybrid polymer electrolytes.

Solid-state polymer electrolytes

A solid-state polymer electrolyte based DSSC is fabricated by solution casting of the polymer electrolyte solution directly onto a dye adsorbed TiO_2 photoanode. In another type of solid-state device, a polymer electrolyte membrane is placed on top of the sensitized TiO_2 film.

Gel based polymer electrolytes

In a classical gel polymer electrolyte based device, a dissolved polymer network with different electrolyte composition is gellified by various means such as plasticizers, co-polymerization, organic gelators, crosslinkers etc. On the other hand, in the modified gel polymer based electrolytes, the device is fabricated by using a gel swollen in a liquid electrolyte. In this method, the liquid electrolyte is entrapped into the polymer

gel matrix. Thus, the problems regarding solvent evaporation and leakage, photo degradation of the photoanode and corrosion of the counter electrode can be eliminated. Gel polymer electrolytes have low vapour pressure, higher conductivity, and excellent thermal stability with long-term durability.[83] They offer exceptional contact and filling between the electrodes. DSSCs fabricated using such electrolytes are known as the quasi-solid state devices.

Hybrid polymer electrolytes

Hybrid polymer electrolytes include both organic and inorganic phases inside the polymer matrix. Various inorganic nanofillers like titanium dioxide (TiO_2)[84], carbon nanotubes,[85] silica (SiO_2)[86] etc. are incorporated into the polymer matrix to form electrolytes. Nanofillers are incorporated in order to improve the mechanical, interfacial and conductivity properties.

In 1883, forty four years after the discovery of the photoelectrochemical cell by Becquerel, Vogel discovered the photosensitivity to longer wavelength with the addition of a dye sensitizer into a silver halide emulsion. The first known DSSC was developed by Grätzel and his group, who applied an organic dye molecule on nanocrystalline TiO_2 as light absorber in 1991[79]. A PCE of 7.1-7.9% was achieved. The role of the I_3^-/I^- redox couple is to assist the regeneration of the dye molecules inside the DSSC. Although, numerous works have been carried out on liquid electrolyte based devices which offer significantly high PCE,[87, 88] these devices have lots of problems such as the sealing problem and photodegradation of electrodes by the solvent present in the liquid electrolyte. Therefore, much work have been devoted to develop solvent free electrolytes.[77, 81]

Generally, any material with p-type semiconducting properties and capable of electron donation to the oxidized dye is considered as the potential substitute for liquid electrolyte. The solvent-free room temperature ionic liquids (RTIL) have been widely studied in DSSC for a long time due to its double role as solvents as well as redox couples.[77] However, a number of pitfalls related to such ionic liquids limit their use in DSSCs. Finally, the concept of polymer based electrolytes came into consideration in twenty years back when Cao et al. for the first time reported the use of polymer

electrolyte in DSSC.[89] In 2004, Kim et al. reported a solid-state polymer electrolyte with PCE of 4.5% by using a low molecular weight polymer, poly(ethylene oxide dimethyl ether) (PEODME) with 1-methyl-3-propylimidazolium iodide (MPII)/iodine (I_2)/fume SiO_2.[86]

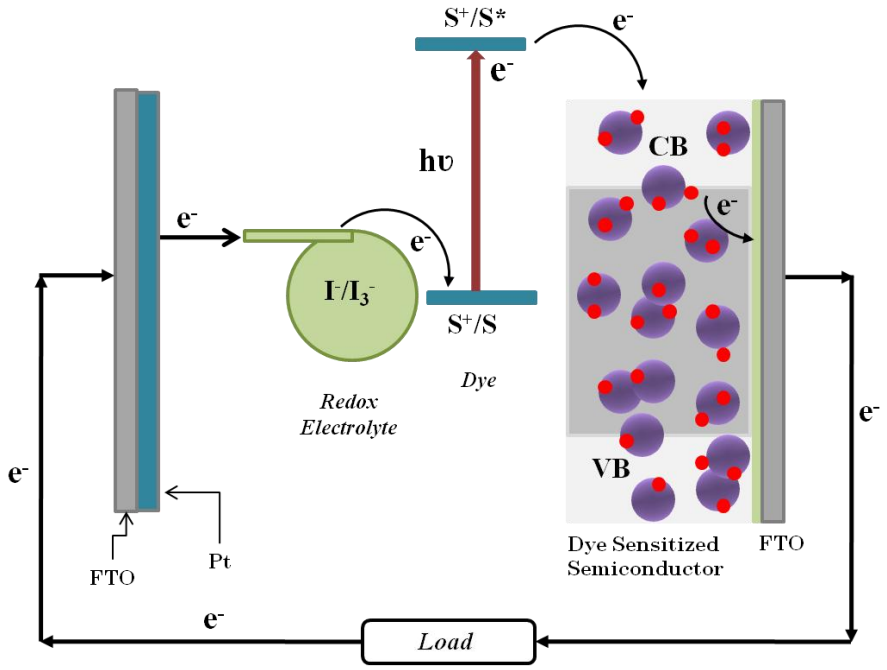

Fig. 1.3 Schematic representation of a hybrid gel polymer electrolyte based DSSC

The polymer electrolytes, obtained from a bio-polymer are considered as an interesting alternative. But efficiency is very low for such devices. For instance, In a solid-state device using an electrolyte membrane consisting of a biopolymer complexed with ammonium and ionic liquid chitosan ammonium iodide (NH_4I)-butyl-methyl imidazolium iodide (BMII), conductivity of $3.43x10^{-5}$ Scm^{-1} is achieved at room temperature.[90] In 2014, the use of a solid state electrolyte is reported in a bio-based polyurethane (PU) complexed with lithium iodide (LiI)/I_2.[80] But efficiency of the device is very low because of the weak contact at the interface of the semiconductor and the electrolyte. However, the UV-cured PU along with the liquid electrolyte LiI/I_2, 1-butyl-3-methylimidazolium iodide (BMImI) and tertiary butyl pyridine (TBP) in 3-methoxypropionitrile (MPN) provides PCE of 6.10%.[91] In 2007, Lan et al. reported the PCE of 3.19% for poly(acrylic acid) (PAA) and poly(ethylene glycol) (PEG) co-polymer when the film is soaked in sodium iodide (NaI)/I_2 electrolyte by swelling technique.[92] The liquid electrolyte is well encapsulated inside the gel through swelling giving rise to a moderate value of ionic conductivity. Thus, the leakage of the liquid

electrolyte can be prevented. Priya et al. deployed the same swelling technique for the preparation of electrospun poly(vinylidenefluoride-co-hexafluoropropylene) (PVDF-HFP) membrane.[93] A significantly high PCE of 7.3% was achieved from the device.

Table 1.3 Performances of several DSSCs utilizing polymer electrolyte under 100 mW cm^{-2} light illumination

Electrolyte	σ ($x10^{-3}$ S cm^{-1})	η (%)	Ref
Solid polymer electrolyte			
PEODME/MPII/I_2/SiO_2	---	4.50	**80**
PU–LiI/I_2	0.74	0.003	**80**
Gel polymer electrolyte			
PU–LiI/I_2–BMImI–TBP	9.80	6.10	**91**
SPE/Chitosan–NH_4I/I_2–BMII (anthocyanin)	0.03	NA	**90**
PAA-PEG–NaI/I_2–TBP (N3 dye)	3.24	3.2	**92**
PVDF-HFP–EC/PC–LiI/I_2–C_6DMII–TBP	0.01	7.3	**93**

*N3-cis-Bis(isothiocyanato) bis(2,2'-bipyridyl-4,4'-dicarboxylato ruthenium(II), EC-ethylene carbonate, PC-propylene carbonate, C_6DMII-1-Hexyl-2,3-dimethylimidazolium iodide

1.3.2 A brief history of hybrid polymer electrolyte

Hybrid polymer electrolyte or nanocomposite based polymer electrolytes are the important matter of discussion as in such electrolytes nanoscale fillers offer improved mechanical, interfacial and conductivity properties. The pioneering work of Scrosati et al. exposed a new direction towards the use of polymer nanocomposite electrolytes in DSSCs.[94] An improved ionic conductivity of the electrolytes have been reported with the addition of inorganic TiO_2 nanoparticles. Polymer electrolytes based on carbonaceous materials, such as single walled carbon nanotubes (SWCNT), multi walled carbon nanotubes (MWCNT) etc. have been extensively studied. Nanotubes are well-dispersed into the polymer matrix thus offering significant improvement in device performance. In a gel electrolyte containing 5 wt% MWCNT, PEG and LiI/I_2, increased J_{sc} is observed with the highest PCE of 0.75%, where the effect on V_{oc} is negligible. However, an excess concentration causes decrease in V_{oc} owing to charge

recombination.[95]

A well-dispersed suspensions of MWCNTs using poly(oxyethylene)-segmented amides and imides (POEM) as dispersants observe a PCE of 6.86% with a 0.25 wt% of MWCNT/POEM.[96] The presence of aromatic as well as amide-imide functionalities in the POEM structure can generate non-covalent bonds, such as π–π stacking interactions with MWCNT and poly(oxyethylene) segments. This allows chelating with Li^+ ions in the electrolyte. Y-Hsun Chang et al. reported the photovoltaic performance of a new electrolyte containing MWCNT/1-(2-acryloyloxy-ethyl)-3-methyl-benzoimidazol-1-ium iodide (AMBImI) well dispersed in the poly(1-(2-acryloyloxy-ethyl)-3-methyl-imidazol-1-ium iodide) (poly(AMImI) electrolyte. The electrolyte offers PCE of 3.55% for 0.5 wt% MWCNT/AMBImI concentration.[97] The high PCE is owing to the higher J_{sc} value as the V_{oc} value remains almost constant. This implies that the presence of MWCNT/AMBImI and MWCNT-poly(AMImI) enhances the diffusion of I_3^- ion in the solid electrolyte that contributes towards improved value of J_{sc}. Similar to carbon nanotubes, other one-dimensional nanoparticles such as nanotubes, nanorods, nanowires can be used for efficient electron transport and also transport of optical excitations.

A hybrid material composed of a metallic nanoparticle immobilized and impregnated into a polymer matrix is known as the metal-polymer nanocomposite film. In such a hybrid material, the individual properties of both the polymer and the metal nanoparticle give rise to some fascinating properties which are very useful in photovoltaic applications. The polymeric host material offers processibility and transparency, at the same time prevents nanoparticle aggregation by immobilizing them into its network. The metal nanoparticles like Au or Ag contribute with their intrinsic optical properties. Due to their contribution towards optical behaviour of the hybrid material, metal nanoparticles are often known as the "optically effective additives".[98] Due to the SPR of Au metal nanoparticles, they observe a strong plasmon band in the visible spectrum which are basically dependent on size and shape of the nanoparticle. This plasmon band offers the useful application of Au nanoparticles in optical sensing. The plasmon band shifts towards longer wavelength as the dielectric constant in the surrounding of the nanoparticle changes. This effect is used for sensing

applications.

In the quasi solid state DSSCs, the concept of hybrid electrolyte made up of Au metal nanoparticles is very new. Till now, numerous works have been devoted to the utilization of Au nanoparticles on the photoanode layer to enhance the photo response of the electrode. For instance, Au nanoparticle embedded TiO_2 electrode strongly absorbs light because of the LSPR thus promoting light absorption of the dye. Consequently, PCE of the cell increases from 2.7% to 3.3% with the use of Au nanoparticles.[88] The DSSCs based on ZnO nanoflowers loaded with Au nanoparticles show a significant enhancement in PCE from 1.6% to 2.5%. The decoration of Au nanoparticles on the ZnO photoanode reduces the recombination centres generally attributed to the oxygen vacancies in the surface layer of ZnO. Moreover, the plasmon mode of Au nanoparticle energetically overlaps with dye absorption zone possibly providing charge into the ZnO nanostructure.[99] The incorporation of Au/SiO_2 core-shell nanoparticle into DSSCs offers plasmon enhanced light absorption and photocurrent generation inside the cell. Here, the core-shell structure acts as the plasmonic light harvesting antennae on the photoanode.[100]

Another study investigated that the core-shell structure of Au/poly(4-vinylpyridine) (Au/PVP) incorporated into the photoanode offers the chemical stability towards I^-/I_3^- electrolyte as well as adhesiveness to dye molecules. This may help in localization of most of the dye molecules in the vicinity of plasmonic nanoparticles, thus offering enhanced optical absorption. Subsequently, PCE increases from 3.3% to 4.3% with the incorporation of Au/PVP core-shell nanoparticles.[101] Similar to other hybrid polymer nanocomposite electrolytes, the addition of Au nanoparticles may facilitate the enhancement of ionic conductivity inside the polymer electrolyte by providing a large active surface area. Thus, it offers excellent electrocatalytic activity for the I_3^-/I^- reaction.[102] Just like MWCNT, one dimensional Au nanoparticles such as nanorods may transport electrons through its different channels that can reduce charge recombination. This results in significant photovoltaic property in the electrolyte. Although numerous literatures are found on the use of metallic Au nanoparticles in quasi solid state DSSCs, however a lot of scope may arise in this field of research.

1.3.3 Gelatin

Bio-degradable polymers, obtained from renewable resources are considered a suitable alternative to liquid electrolytes. These are abundant in nature, biocompatible, biodegradable, environmentally benign, non-flammable and have superior mechanical and electrical properties.[103] Numerous examples are found on quasi solid state DSSCs where these polymers are used as the gel electrolyte. The cyanoethylated hydroxypropyl cellulose (CN-HPC) polymer gel electrolyte based on LiI/I_2 and 1-methyl-3-hexylimidazolium iodide (MHII)/I_2 as the I^-/I_3^- redox couple provides PCE of 7.4% for triphenylamine dye (SD2) and 7.55% for ruthenium dye, di-tetrabutylammonium-cis-bis(isothiocyanato)bis(2,2'-bipyridyl-4,4'-dicarboxylato) ruthenium(II) (N719). The PCE is increased by 94% of those with the conventional liquid electrolyte.[104]

A biopolymer electrolyte comprised of another cellulose derivative, carboxymethyl cellulose (CMC) shows a significant ionic conductivity of 5.77×10^{-4} S cm^{-1} at ambient temperature with 20 wt% of ammonium acetate (CH_3COONH_4). The biopolymer electrolyte film also exhibits electrochemical stability up to 2.5 V which has unveiled the potential of the electrolyte in DSSC applications.[105] The microfibrillated cellulose (MFC)-based polymer electrolyte membrane shows better photovoltaic performance (PCE: 7.03%) than CMC-based gel-polymer electrolyte (PCE: 5.18%). In case of MFC, curing of the gel is very fast which helps in maintaining a homogeneous dispersion of the filler. The interpenetration between the polymer matrix and network of fibres is excellent. After activation in the redox electrolyte a free-standing, easy hold, non-tacky and flexible membrane is obtained.[106] An all-solid-state DSSC using a new carbohydrate polymer electrolyte system containing Arrowroot biopolymer doped with potassium iodide (KI) offers a PCE of 0.63% at 1 sun condition. Arrowroot (Maranta arundinacea) is a biopolymer containing about 23% starch (20 to 25% amylose and 75 to 80% amylopectin) and is a low-cost material. It does not require elaborate apparatus to manufacture.[107] A novel quasi solid state DSSC based on agarose gel electrolyte doped with KI shows PCE of 0.54% at 100 mW/cm^2 light intensity. The doping of KI provides the additional charge carriers (cations/anions) which enhances overall conductivity.[108] A gel polymer electrolyte is prepared by using phthaloylchitosan with tetrapropylammonium iodide (Pr4NI) salt. The quasi solid state DSSC fabricated with the electrolyte exhibits a

maximum efficiency of 3.71% when salt ratio of Pr4NI:LiI is 2:1. The cell obtains J_{sc}, V_{oc} and FF of 7.25 $mAcm^{-2}$, 0.77V and 67% respectively.[109]

Gelatin is one of the natural polymers that has the ability to form new electrolyte materials for quasi solid state DSSCs. It is abundant and biodegradable, has low-cost, has excellent film-forming ability, is non-toxic and can form transparent solutions with high viscosity.[110, 111] Generally, gelatin films are obtained by solubilization, heat or dehydration of collagen which leads to distortion of a partial helix of this macromolecule. However, by using a crosslinker such as glutaraldehyde, formaldehyde or glioxal the functional properties of gelatin can be improved.[112, 113] Vieira et al. developed three different electrolytes containing acetic acid[114] and lithium perchlorate ($LiClO_4$).[115] based on crosslinked gelatin with formaldehyde, and plasticized with glycerol. The amount of acetic acid influences the proton conduction. For instance, the ionic conductivities of proton-conducting polymer electrolytes based on gelatin and acetic acid at room temperature and at 80 °C are $4.5x10^{-5}$ Scm^{-1} and $3.6x10^{-4}$ Scm^{-1} respectively with 26.3 wt% acetic acid concentration.[110] The ionic conductivity as a function of temperature exhibits Arrhenius behaviour and the values of activation energy decreases by increasing the acetic acid concentration. The results suggested that the electrolyte is very attractive for electrochemical device applications. Similarly, the amount of $LiClO_4$ influences the electrolyte conductivity thus providing a maximum value for 7.9 wt%. For the optimum salt concentration the ionic conductivity increases from $1.5x10^{-5}$ Scm^{-1} at room temperature to $4.9x10^{-4}$ Scm^{-1} at 80 °C. Crosslinked gelatin hydrogel electrolytes (GHEs) with semi-interpenetrating network are prepared using aqueous glutaraldehyde as the crosslinker and with varying concentration of sodium chloride (NaCl). Ionic conductivity of the GHEs increases from 10^{-3} to 10^{-1} S cm^{-1} as the dopant concentration is increased from 0 to 3 N. On the other hand, with increase in the concentration of gelatin and glutaraldehyde precursor solutions, ionic conductivity of the GHEs is decreased.[111]

M.M. Silva et al. investigated the electrochemical properties of a series of electrolytes with the incorporation of controlled quantities of $LiClO_4$ into the gelatin host matrix. The gelatin host has the ability to dissolve quantities of $LiClO_4$ without the formation of crystalline lithium-polymer complexes. These solid state electrolytes offer excellent

mechanical and electrochemical properties.[116] Proton-conducting gel polymer electrolytes based on gelatin and acetic acid plasticized with glycerol are obtained by Amal Al-Kahlout et al. in 2010.[117] The electrolyte film shows an 80% high transparency above 450 nm, a predominantly amorphous state and good surface uniformity. The proton conductivity is found to follow Vogel-Tamman-Fulcher (VTF) behaviour with the temperature and it increases from $4.5x10^{-5}$ Scm^{-1} at room temperature to $3.6x10^{-4}$ Scm^{-1} at 80 °C with the plasticizer (glycerol) concentration of 28%.

Gelatin-based electrolytes are synthesized with varying concentration of zinc triflate ($Zn-(CF_3SO_3)_2$).[118] It is observed that the electrolyte gelatin/$Zn-(CF_3SO_3)_2$ with 7.01% Zn salt concentration shows the highest ionic conductivity of $4.60x10^{-7}$ Scm^{-1} at 95 °C. All analyzed samples show good mechanical, thermal and electrochemical properties, good transparency and a useful adhesive function. Another investigation shows that the highest room temperature conductivity of the gelatin electrolyte system, doped with 1-ethyl-3-methylimidazolium acetate (EMIM Ac) is $1.18x10^{-4}$ Scm^{-1} which follows the VTF conducting type model.[119] Gelatin and lithium tetrafluoroborate ($LiBF_4$) based polymer electrolytes are prepared. It is found that the effect of plasticizer on the ionic conductivity of the electrolyte is much more important than the effect of lithium salt or the effect of the interaction of both variables. For instance, a remarkable ionic conductivity of 2.29×10^{-5} Scm^{-1} is observed for 58.8 wt% glycerol,[120] while for 3.7 wt% Li salt it is only 1.4×10^{-5} Scm^{-1}.

1.3.4 ZnO photoanode for DSSCs

ZnO is a binary transition metal oxide with wide band gap (~3.3 eV). It preferentially crystallizes in the hexagonal wurtzite phase. Fabrication of the nanoparticle is very simple and easy with comparatively low-production costs. ZnO has the conduction band edge almost close to that of TiO_2 (ca -4.4 eV). In addition to that, it has higher electron mobility in the bulk (200-300 $cm^2V^{-1}s^{-1}$) than TiO_2 (0.1 $cm^2V^{-1}s^{-1}$) and less toxicity. Therefore, ZnO has been extensively studied in DSSCs as a relevant alternative to TiO_2. The first work on visible sensitization of ZnO by merocyanine dye was investigated four decades ago.[121] The first photovoltaic properties of ZnO-based

photoelectrochemical devices are reported later on.[122-124] Various groups investigated the electronic properties of nanostructured ZnO electrodes and compared with the TiO_2 electrodes. It is found that electron lifetime in nanocrystalline ZnO films is longer than in TiO_2 as there are fewer traps in the nanostructure.[125, 126] Moreover, in reverse bias conditions, charge recombination is found to be slightly accelerated in ZnO compared to TiO_2 electrodes that provides a significantly smaller value of V_{oc}.[126] Furthermore, ZnO faces difficulty in sensitization because of the intrinsic instability of the metal oxide in acidic dye solution. Therefore, the main drawback of such electrode based DSSC is its lower efficiency compared to TiO_2.[127] But the possibility of using various soft synthetic methodologies, such as sol-gel hydrolysis at low temperature, solvothermal method has driven much effort towards their development.

K. Keis et al. reported 5% efficient DSSC based on ZnO electrodes using a liquid electrolyte, 0.5M LiI/50 mM I_2 in 3-methoxypropionitrile and N719 ruthenium dye.[87] In 2000, O'Regan et al. for the first time investigated the use of electrodeposited porous ZnO electrodes for solid state DSSCs, where a solid electrolyte, copper(I) thiocyanate (CuSCN) and a ruthenium-based dye have been used.[128] Recently, nanocrystalline ZnO photoanodes grown at low temperature from solution offer a modest PCE of 0.5% using a molecular hole transporter 2,2,7,7-tetrakis-(N,N-di-p-methoxyphenylamine)-9,9-spirobifluorene (spiro-OMeTAD) and N719 dye.[129] Anisotropic ZnO nanostructures such as nanorods, nanowires, nanotubes etc. have been recently implemented in DSSC in place of nanoparticles in order to achieve better transport properties. In a DSSC, the morphology of the nanoparticle in the photoanode affects on electron transport and consequently on efficiency of the device.

The conventional isotropic, i.e., spherical nanoparticle film shows some drawbacks which may be detrimental to efficient electron transport. A nanoparticle film undergoes a trapping and de-trapping process. As a result of such process the injected electrons are captured by the trap states and may again be thermally emitted back to the conduction band. This may cause energy loss to the injected electrons. A nanoparticle film has lots of grain boundaries which may be responsible for this energy loss.[130] Another factor arises in terms of diffusion length. In a nanoparticle film, the typical electron diffusion length is 10-14 μm. That is why; an optimal thickness of the

film should be around ten several micrometers. Otherwise, a thicker film may act as a barrier to the dye adsorption. However, recently one dimensional nanostructures (viz.,

Table 1.4 Summary of photovoltaic parameters (J_{sc}, V_{oc}, FF and PCE) corresponding to both liquid state and solid-state DSSCs based on ZnO photoanode

	J_{sc} ($mA.cm^{-2}$)	V_{oc} (V)	FF %	η %	Ref
Conventional liquid-state DSSC approaches					
FTO/ZnO/N719/LiI:I_2:4-TBP/Pt/FTO	1.3	0.56	68	5.0	[87]
Liquid state DSSC based on 1-D ZnO					
FTO/ZnO NW/N719/tetrabutylammonium iodide:I_2:4-TBP/Pt/FTO	1.62	0.74	38	0.5	[133]
FTO/ZnO NT/N719/ LiI:I_2:4-TBP/Pt/FTO	3.2	0.68	58	1.2	[135]
AAO/ZnO NT: AZO/N719/LiI:I_2:tert-butylpyridine/Pt/FTO	3.3	0.74	64	1.6	[136]
FTO/ZnO NW:TiO_2 NP/N719/LiI:I_2:4-TBP: 1-hexyl-3-methylimidazolium iodide/Pt/FTO	3.54	0.60	37	0.8	[139]
FTO/sponge like ZnO/N719/Iodolyte AN50/Pt/FTO	16.63	0.63	64	6.7	[140]
FTO/ZnO NW:ZnO NP/mercurochrome/ tetra-n-propylammonium iodide:I_2/Pt/FTO	8.33	0.58	58	2.8	[141]
FTO/ZnO NW:ZnO NP/N3/Pt/FTO	15.16	0.61	46	4.2	[142]
FTO/ ZnO:polyvinyl acetate composite nanofiber mats/N719/: BMII:I_2:guanidinium thiocyanate:4-tert-butylpyridine/Pt/FTO					[143]
Solid-state DSSC approaches based on ZnO					
FTO/porous ZnO/P-Ru dye/CuSCN/Au/FTO	4.50	0.55	57	1.5	[128]
FTO/porous ZnO/N719/spiro-OMeTAD/Au/FTO	2.05	0.39	53	0.5	[129]

*N719-cis-bis(4,4′-dicarboxy-2,2′-bipyridine)-bis(isothiocyanato)ruthenium (II), NW-Nanowire, NT-Nanotube, NP-Nanoparticle, AAO-Anodic aluminium oxide, AZO-Aluminium doped zinc oxide, P-Ru dye-Phosphonated ruthenium polypyridyl dye, BMII-1-butyl-3-methylimidazolium iodide, 1-D-one dimensional, Iodolyte AN50-electrolyte (Solaronix)

nanorods, nanowires, nanotubes) have been shown to minimize such demerits of conventional nanoparticle films. They offer a direct pathway for electron transport, thus resulting in larger diffusion length than in the nanoparticle films.[131, 132]

The first report on one-dimensional ZnO nanoparticles is demonstrated in a liquid electrolyte based DSSC. Here, the electron diffusion coefficients are two orders of magnitude higher than the conventional nanoparticle film and also offer better ability for charge collection.[133, 134] ZnO nanotubes are also considered beneficial as a photoanode due to large amount of dye loading at both the outer and inner surfaces of the nanotube as well as light scattering effects. However, such nanostructures are suffering from relatively low efficiency, generally ~1.2-1.6%.[135-138] Recently, hybrid nanostructures composed of one dimensional ZnO and other nanostructures have attracted lots of attention in photovoltaic research. X. Gan et al. investigated the photovoltaic performance of dye sensitized solar cells by using a hybrid ZnO nanowire/TiO_2 nanoparticle as photoanode. An overall PCE of 0.79% is obtained.[139] Highly efficient dye sensitized solar cells, with PCE 6.67% are obtained by using sponge like ZnO nanostructures as photoanode.[140] Similarly, other hybrid structures are observed which offer remarkable photovoltaic properties.[141-144] However, all the works related to one dimensional ZnO nanostructures have investigated the photovoltaic performance of only liquid electrolyte based DSSCs. Till date, a very few literatures are found on the utilization of one-dimensional ZnO photoanodes in solid state or quasi-solid state DSSCs.

1.4 Synthetic routes of nanocrystals

1.4.1 Hydrothermal method of synthesis of ZnO nanorods

The term 'hydrothermal' is purely originated from the geology, as it was first described by the British geologist, Sir Roderick Murchison (1792-1871). The hydrothermal process was defined by him as the action of water at elevated temperature and pressure which brings about changes in the earth's crust leading to the formation of various rocks and minerals. It is a heterogeneous reaction in presence of aqueous solvents or mineralizes under high pressure and temperature conditions to dissolve and re-crystallize materials that are relatively insoluble under ordinary conditions.

Hydrothermal method is one of the efficient bottom-up approaches of synthesis of anisotropic nanoparticles. In this method, an aqueous solution of the precursor is placed into a teflon-coated stainless steel autoclave and sealed, followed by maintaining the temperature normally at 100-200 °C for 10-40 h. The synthesized product is then collected from the walls of the reaction chamber, centrifuged, washed and dried. This process is successfully utilized to get nanorods of various materials, such as CdS,[145] TiO_2,[146] ZnO[147, 148] etc.

Hydrothermal method is one of the most energy-efficient and economical methods for the synthesis of ZnO nanorods. This process has numerous advantages over other growth processes such as low cost, use of simple equipment, large area uniform production, environmental friendliness, less hazardous and catalyst-free growth. The method induces anisotropic crystal growth in an aqueous solution. In this process, properties of nanoparticle such as morphology and size can be controlled easily by adjusting the reaction temperature, time and concentration of precursors. It is a surface independent process thus providing good control over the morphology of the nanostructure grown.

The first report on hydrothermal synthesis of ZnO nanorods was provided by Vayssieres et al.[149] An equimolar solution of zinc nitrate and hexamine allows the epitaxial growth of ZnO nanorods on various substrates using small ZnO crystallites as seeds. A surfactant, such as cetyl trimethyl ammonium bromide (CTAB) is used to modify and control the size and morphology of the synthesized nanoparticle in aqueous solution. Zhai et al. used CTAB as the surfactant to prepare ZnO nano and micromaterials under solvothermal condition.[148] Using a reverse microemulsion and hydrothermal method, ZnO nanowires are synthesized.[150] ZnO nanorods with different sizes and shapes are successfully synthesized via a simple hydrothermal route, using zinc acetate and CTAB as the reactants. The synthesized ZnO nanorods proved to be excellent candidates for gas sensors.[151]

1.4.2 Seeded growth method of synthesis of Au nanorods

The seed-mediated growth method is one of the most efficient and versatile methods for the synthesis of high-quality noble metal nanocrystals. A typical seeded growth

method involves the preparation of noble metal seed nanoparticles and their subsequent growth into metal nanocrystals in a solution containing metal precursors, reducing agents, and shape-directing reagents.[152] The most commonly used shape directing reagents are cationic surfactants such as CTAB and cetylpyridinium chloride ($C_{16}PC$).[153] The synthesis of metal nanocrystals can be divided into two major categories depending on the temporal and spatial differences of the nucleation and growth stages.[154]

- *Homogeneous nucleation*: In such nucleation, both the nucleation and growth occur in the same reaction medium. The seed nanoparticles are generated in-situ.
- *Heterogeneous nucleation*: In such nucleation, the seed nanoparticles are pre-synthesized followed by addition of the seeds into a growth solution to allow further growth into metal nanocrystals.

The main requirement in the formation of metal nanocrystals with narrow size and shape distribution is the temporal separation of the nucleation and growth stage.[155] In view of heterogeneous nucleation, the seed-mediated growth method can fulfil this requirement as the process can separate the nucleation and growth step, thus offering better control over size, size distribution and shape evolution of metal nanocrystals. Due to the high controllability regarding the size and shape distribution, this method is especially efficient in providing mechanistic insights into the growth of metal nanocrystals.

The seed-mediated growth method has become one of the most resourceful methods for the synthesis of anisotropic metal nanocrystals in last 10 years. The Murphy and El-Sayed groups started this method to control the shape of different metal nanocrystals, mainly Au and Ag. Long Au nanorods with penta-twinned structures are yielded by a three-step seeding method developed by the Murphy group.[156] It is observed that the aspect ratio of the Au nanorods is proportional to the length of the surfactant, alkyl trimethyl ammonium bromide (C_nTAB) chain. The surfactant binds as a bilayer to the growing nanoparticle and assists in nanoparticle elongation via a mechanism proposed by the group as the "zipping" mechanism.[153] Murphy and his co-workers also studied the effect of seed size on length of the nanorods. It is found that

as the size of the seeds decreases, the aspect ratio of the nanorods, increases to a large extent. This effect is more pronounced in negatively charged seeds compared to positively charged ones.[157] The El-Sayed group designed a one-step route towards the formation of single-crystalline Au nanorods with 100% yield.[158] Thus, these two scientist groups introduced the seed-mediated growth process for the synthesis of anisotropic metal nanocrystals with both high quality and reproducibility.

1.5 Synthesis of polymers

There are number of techniques of polymerization of PVK, P3AT which includes radical chain polymerization, oxidative coupling etc. In radical chain polymerization, the polymerization is initiated by free radicals formed as a consequence of thermal or photochemical decomposition. An initiator, like benzoyl peroxide (BPO) or 2,2´-azo-bis-isobutyrylnitrile (AIBN) initiates the reaction. In the oxidative coupling method, the monomer solution in a suitable solvent is oxidatively polymerized in presence of an oxidizing agent, like ferric chloride ($FeCl_3$). This technique is very effective in the polymerization of 3-alkylthiophene (3AT). 3AT monomer can produce radical cations with spin-density, pre-dominantly in the 2 and 5-positions of the thiophene, due to the oxidation in presence of $FeCl_3$. It is worth-mentioning that in such polymerization technique, the coupling occurs with no region-chemical control and hence produces structurally irregular polythiophenes, denoted as regio-irregular P3AT. Since the π-conjugation is somewhat lost due to this irregular structure, this leads to comparatively reduced electrical properties. But still the complicated and expensive synthesis conditions of regio-regular polythiophenes always prefer the oxidative coupling to synthesize the polymer in laboratory scale.

It is known that 9-vinylcarbazole (NVK) is a very reactive monomer towards radical, cationic and charge transfer polymerization. It can stabilize the electron-deficient centres by resonance involving the non-bonding electron pair on the nitrogen atom in the carbazole ring.[159] The free-radical polymerization of NVK, carried out in dispersion and suspension has a considerable commercial interest. The process is extremely facile when the monomer contains no impurities. In presence of the impurity, the polymerization process is retarded and the yield becomes very low.[159] The polymerization reaction is very fast in presence of BPO or AIBN as initiator of the

order of 94.5 ± 2.4 sec^{-1} as compared to 9.4 ± 0.4 sec^{-1} for styrene.[160] An oxidation route to the synthesis of soluble polycarbazole has been applied by Rajender Boddula et al. using BPO as the initiator and the yield is 69%.[161] AIBN has also been used elsewhere as an initiator.[162]

The oxidative coupling polymerization for the synthesis of P3AT does not require any leaving groups and it is very easy to remove the by-product from the resulting polymers. Therefore, the process can form the polymer in large-scale. The coupling method using $FeCl_3$ is very effective in the synthesis of regio-irregular P3AT due to its easy accessibility.[68, 163] However, in some rare cases regio-regular polymer can also be formed.[164] Although many groups used other halides and many other materials as oxidants, Fe (III), Mo (IV) and Ru (III) chlorides are most effective.[165] The mechanism of polymerization of 3-alkylthiophene in presence of $FeCl_3$ was adopted by Niemi et al.[166] Likewise, a number of researchers have synthesized various derivatives of P3AT and optimized the reaction conditions.[167, 168]

1.6 Preparation of gelatin hydrogel

A hydrogel is defined as a three dimensional polymer network that is hydrophilic and water insoluble. Hydrogels are highly absorbent natural or synthetic polymers which take in and keep huge quantities of fluids especially 99.9% of water. Generally, hydrogels are prepared from hydrophilic monomers, still sometimes to regulate the properties for specific applications hydrophobic monomers are used in the synthesis. Conventional polymerization techniques including bulk, solution and suspension polymerization are used to synthesize the gel. In general, the hydrogel formation includes three integral parts particularly monomer, initiator and crosslinker. After the polymerization, the polymer is allowed to crosslink in order to form the hydrogel network. There are two types of crosslinking procedures: physical crosslinking and chemical crosslinking.

In the physical crosslinking, physical interactions such as ionic interactions, hydrogen bonding interactions, hydrophobic interactions etc. exist between polymer chains. Conversely, covalent interactions are present between polymer chains in chemically crosslinked hydrogels. These interactions include polymerization (viz., acryloyl

group), radiation (viz., γ-ray), small-molecule crosslinking in presence of another molecule (viz., glutaraldehyde) etc. Due to the presence of chemical crosslinks such as tie-points and junctions or physical crosslinks such as entanglements and crystallites, the crosslinked hydrogels are insoluble in nature and the high water content makes the material biocompatible. The hydrogels exhibit thermodynamic compatibility due to which the polymer is swelled in aqueous media and more or less in other fluid medium. This property is suitable to form a gel electrolyte.

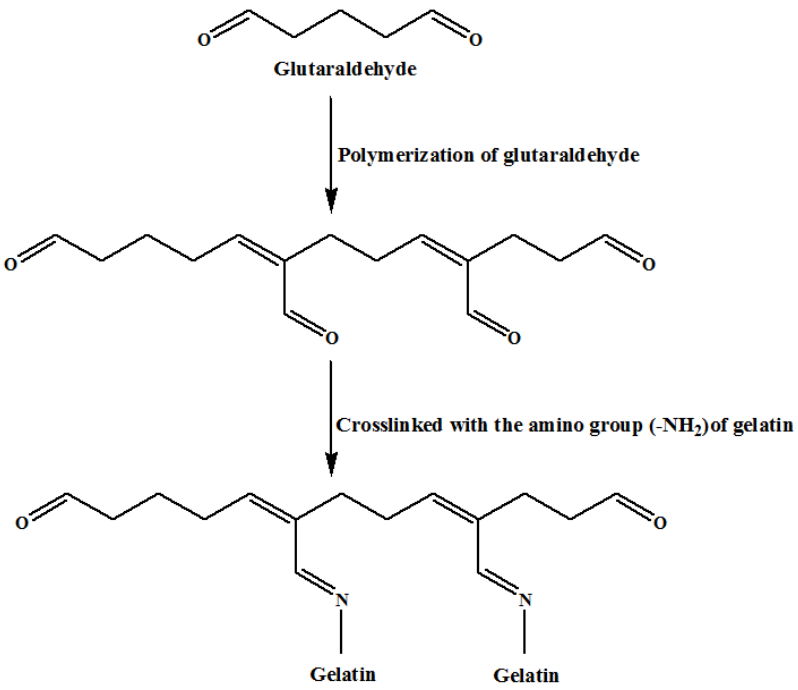

Scheme 1.1 Crosslinking of gelatin with glutaraldehyde

A polymer with pendant functional groups such as hydroxyl (OH), carboxyl (-COOH) and amino ($-NH_2$), can be crosslinked by forming covalent bonds between polymer chains by the reaction of functional groups with complementary reactivity such as an amine-carboxylic acid or an isocyanate-OH/NH_2 reaction etc. For instance, -OH group containing water soluble polymers can be crosslinked by an aldehydic crosslinker, glutaraldehyde.[169] However, in such crosslinking certain experimental conditions such as low pH, a quencher, high temperature etc. are to be applied. Alternatively, the same crosslinker is very much effective even under mild conditions in the crosslinking of various amine containing polymers in which Schiff bases are formed. Glutaraldehyde

is specially designed for the synthesis of crosslinked proteins, particularly gelatin[170, 171] As a commercially available and low cost material with high reactivity, glutaraldehyde has found wide application as a crosslinker in various fields such as biomedical, pharmaceutical, chemical sterilization etc.[172, 173] It rapidly reacts with the amine group at around neutral pH and forms chemically and thermally more stable crosslinks[172] [Scheme 1.1]. A lot of works have been reported on gelatin hydrogel crosslinked by glutaraldehyde or other crosslinking agents.[174-177]

1.7 Synthesis of polymer nanocomposites

Since civilization, in search of more efficient materials for specific purposes, people were trying to make modified materials. An example of a man-made nanocomposite is the Maya blue which combines the resistance of the inorganic clay palygorskite with organic pigment blue indigo.[178] The concept has been industrially started in 1940s in some companies like Toyota, Dupont, Dow Corning and others. Some examples of industrial nanocomposite products are paper, paints, coupling agents etc.[179, 180] Polymer nanocomposites can be defined as the composites with at least one phase in nanometer range. The incorporation of inorganic nanoparticle into the polymer network offers a huge surface area that increases the interaction between the nanoparticle and the polymer. Consequently, they offer improved properties than their individual counterparts.

Two methodologies have been applied in the synthesis of polymer nanocomposites: bottom-up and top-down. In the previous approach, precursors are used to form the desired structures from the nanometer level. Bottom-up processes include chemical processes, such as, sol-gel, chemical vapour deposition (CVD), template synthesis or spray pyrolysis. In the latter approach, the bulk material is allowed to break into smaller pieces to form the desired product. In the synthesis of polymer nanocomposites three ways have been employed. The first one consists of mixing of the nano-filler and the polymer in solution or in melt.[181] The second includes in-situ polymerization in presence of the pre-synthesized[182] or in-situ synthesis of nanoparticles in presence of the polymer.[183] The last one is based on in-situ formation of both the nanoparticle and the polymer. Except the first one, the other two ways follow the bottom-up approach.

Numerous research have been carried out to study the photovoltaic performance of polymer nanocomposites based on P3AT[68, 163, 96] and PVK.[159, 184]

In the preparation of polymer nanocomposites based hydrogels, the nanofiller is added into the polymer gel solution and mixed thoroughly by ultrasonication followed by addition of the crosslinker. Crosslinking allows the formation of the nanocomposite based hydrogel which can be utilized as a polymer electrolyte.[185]

1.8 Photovoltaic device characterization

The photovoltaic performance of a fabricated solar cell can be measured using the photocurrent density-voltage (J-V) characteristics [Fig. 1.4].

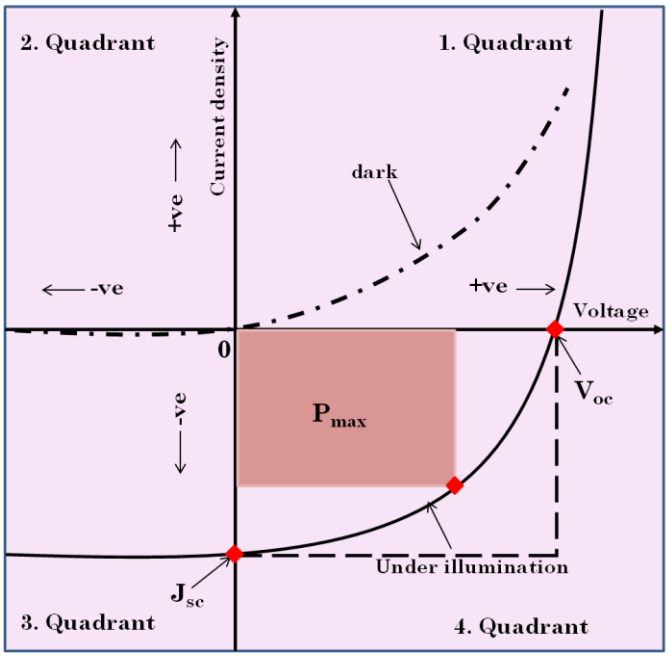

Fig. 1.4 J-V characteristics of a typical photovoltaic device

The photovoltaic characteristic of a typical photovoltaic cell can be seen in the fourth quadrant of the J-V curve. From the voltage dependent J-V curve, certain parameters can be measured which are summarized in the following:

- *Maximum power (P_{max})*: The maximum power can be measured by the maximum product of J (current density= current (I)/active area of the device) and V, that can be obtained amongst the data points in the fourth quadrant.
- *Short circuit current density (J_{sc})*: The short-circuit current (I_{sc}) is the current through the solar cell when cell is short circuited; i.e., when the voltage across

the solar cell is zero. I_{sc} per unit active area of the cell is known as the short circuit current density, J_{sc}.

- *Open circuit voltage (V_{oc})*: The open circuit voltage (V_{oc}) is defined as the maximum voltage obtained from the cell when the current is zero. This corresponds to the amount of forward bias on the solar cell due to the bias of the solar cell junction with the light-generated current.
- *Fill factor (FF)*: In case of a solar cell, the maximum current and voltage are obtained from I_{sc} and V_{oc} respectively. However, at both of these operating points, the power from the solar cell is zero. The fill factor (FF) is a parameter which, in conjunction with V_{oc} and I_{sc}, determines the maximum power from the solar cell.

$$\text{Fill factor, FF} = \frac{J_{max}.V_{max}}{J_{sc}.V_{oc}} \qquad \text{Eqn. 1.1}$$

$$\text{Maximum power, } P_{max} = J_{max}.V_{max} = J_{sc}.V_{oc}.FF \qquad \text{Eqn. 1.2}$$

- Photo conversion efficiency (PCE, η): The Photo conversion efficiency, PCE of a solar cell is determined as the fraction of incident power which is converted to electricity and is defined as:

$$\eta = \frac{P_{max}}{P_{in}} = \frac{J_{sc}.V_{oc}.FF}{P_{in}} \qquad \text{Eqn. 1.3}$$

Here, P_{in} is the power of the incident light.

In order to compare efficiencies of solar cells, solar radiation standards have been defined in the past. In recent times, the most common standard is the air mass 1.5 (AM1.5) spectrum which can be achieved by a commercially available solar simulator. The common input power for efficiency calculations is 1 kW/m^2 or 100 mW/cm^2.

Incident photon conversion efficiency (IPCE): The incident photon conversion efficiency (IPCE) is a measure of the ratio of the photocurrent versus the rate of incident photons as a function of wavelength. IPCE can be expressed in terms of the efficiencies for photon absorption/charge excitation and separation (η_{e^-/h^+}), charge transport within the solid to the solid-liquid interface ($\eta_{transport}$) and interfacial charge transfer across the solid-liquid interface ($\eta_{interface}$).

1.9 Scope and objectives

Recently, conjugated polymer nanocomposites based hybrid BHJ solar cells have grabbed intensive research interest due to their ease of fabrication, light weight, flexibility, disposability and comparatively low cost. The active layer of a BHJ consists of a nanoscale blend of donor and acceptor materials, where the conjugated polymer acts as the donor and the nanofiller acts as the electron acceptor. As a donor material, a low band gap conjugated polymer with high photo absorption ability plays an efficient role. For this purpose, polythiophene with long alkyl side chain serves a significant role, as the polymer absorbs light in the visible range and the alkyl side group offers better solubility of the polymer so that the fabrication becomes easier. Recently, there has been growing research interest on PVK as a donor material due to a lot of virtues related to the structure including easy formation of relatively stable radical cations, high thermal and photochemical stability etc. The device performance of the fabricated devices can be tailored by changing the anisotropy of the nanofillers. Generally, one-dimensional nanostructures such as nanorods, nanotubes, nanowires etc. attain preferable utilization in solar cells as the structures provide a continuous and one-dimensional path for charge transport thus reducing the charge recombination inside the active layer. The metallic and semiconducting nanoparticles play different role in this regard. Nanocrystalline inorganic semiconductors such as ZnO have numerous advantages as an electron acceptor including high electron mobility, high electron affinity, significant chemical and physical stability etc. A plasmonic metallic nanoparticle exhibits SPR in the visible and near infra-red region. Therefore, by incorporating such nanoparticles into a hybrid BHJ device the enhancement of the total light absorption inside the BHJ becomes possible.

Another important class of polymer based hybrid photovoltaic device is the quasi solid state DSSCs employing polymer nanocomposites based gel electrolytes. A polymer electrolyte can substitute the liquid electrolyte in DSSC which is suffering from leakage and durability issues. Hybrid polymer electrolyte based on polymer nanocomposite gel electrolytes are important in the sense that the nanoscale fillers offer improved mechanical, interfacial and conductivity properties to the electrolyte. Owing to numerous advantages related to gelatin as a natural polymer including non-

toxicity, low-cost, excellent film-forming ability etc., gelatin has the ability to form new electrolyte materials for quasi solid state DSSCs. From previous studies it is found that one-dimensional nanofiller, such as carbon nanotubes, gold nanorods etc. offer significant electron transport through the continuous channel of the nanostructure thus reducing the charge recombination inside the electrolyte. However, Au nanorods are still an area of under consideration as very few works have been done on these nanofiller. Moreover, ZnO nanoparticle photoanode can be used as a relevant alternative to TiO_2 in DSSCs because of the ease of fabrication, low production cost, higher electron mobility and less toxicity than TiO_2. One-dimensional ZnO photoanodes such as nanorods, nanowires, nanotubes are attracting recent interest as they offer a direct path for electron transport, thus resulting in larger diffusion length than in the spherical nanoparticle films. Still a very few works have been done on one-dimensional ZnO photoanodes in quasi-solid state DSSCs.

Motivated from the ongoing discussions, the following objectives are set for the present thesis.

Objectives of the present investigation

- To synthesize metallic and semiconductor anisotropic nanoparticles, viz., nanorods and study of their growth mechanism by changing various reaction parameters.
- To synthesize different sets of polymer nanocomposites by incorporating the pre-synthesized nanorods into a low band gap conjugated polymer matrix.
- To synthesize polymer nanocomposite based hydrogel by immobilizing the pre-synthesized nanorods into a natural polymer gel.
- To fabricate different sets of BHJ solar cells using the conjugated polymer nanocomposite material as the active layer.
- To fabricate different sets of quasi solid state DSSCs using the nanocomposite based hydrogel as the polymer electrolyte and to replace the conventional TiO_2 photoanode by the synthesized semiconductor.
- To characterize the prepared nanocomposites and to evaluate the performance characteristics of the fabricated devices.

Plan of work

To fulfill the above objectives the following plans of work have been adopted.

- Synthesis of different aspect ratio ZnO nanorods by a hydrothermal method.
- Synthesis of various aspect ratio Au nanorods by a seeded growth method.
- Synthesis of poly(9-vinylcarbazole) (PVK) and its nanocomposites with different aspect ratio ZnO and Au nanorods.
- Synthesis of poly(3-octylthiophene) (POT) and its nanocomposites with different aspect ratio ZnO nanorods.
- Synthesis of gelatin hydrogel and its nanocomposite based hydrogels using the pre-synthesized Au nanorods and commercially available MWCNTs.
- Fabrication of different sets of BHJ solar cells using the PVK and POT based nanocomposite material as the active layer.
- Fabrication of different sets of quasi solid state DSSCs using the gelatin based nanocomposite hydrogel as the polymer electrolyte and to replace the conventional TiO_2 photoanode by the synthesized ZnO nanorods.
- Characterization of the nanocomposites by Fourier transform infra-red (FT-IR), X-ray diffractometer (XRD), scanning electron microscopy (SEM), energy dispersive X-ray spectroscopy (EDX), transmission electron microscopy (TEM), ultraviolet-visible (UV-visible), photoluminescence (PL), thermogravimetric analysis (TGA), differential scanning calorimetry (DSC), cyclic voltammetry (CV) and electrochemical impedance spectroscopy (EIS).
- Evaluation of the performance characteristics of the fabricated devices under simulated AM 1.5 illumination at 100 mW/cm^2.

Reference

1. Andrade, L., Ribeiro, H.A. & Mendes, A. Dye-sensitized solar cells: an overview, in *Encyclopedia of Inorganic and Bioinorganic Chemistry*, 2011, 1-20.
2. Li, B., et al. *Sol. Energ. Mat. Sol. Cells* **90**, 549-573, 2006.
3. India Energy Portal. http://www.indiaenergyportal.org/subthemes.php?text=solar
4. Becquerel, A.E. *Compt. Rend. Acad. Sci.* **9**, 145-149, 1839.
5. Becquerel, A.E. *Compt. Rend. Acad. Sci.* **9**, 561-567, 1839.
6. This Month in Physics History, April 25, 1954: Bell Labs Demonstrates the First Practical Silicon Solar Cell. https://www.aps.org/publications/apsnews/200904/physicshistory.cfm
7. Li, G., et al. *Nat. Photonics* **6**, 153-161, 2012.
8. Gu¨nes, S., et al. *Chem. Rev.* **107**, 1324-1338, 2007.
9. Tang, C.W. *Appl. Phys. Lett.* **48**, 183-185, 1986.
10. Sariciftci, N.S., et al. *Science* **258**, 1474-1476, 1992.
11. Kraabel, B., et al. *Chem. Phys. Lett.* **213**, 389-394, 1993.
12. Halls, J.J.M., et al. *Nature* **376**, 498-500, 1995.
13. Yu, G., et al. *Science* **270**, 1789-1791. 1995.
14. Peet, J., et al. *Nat. Mater.* **6**, 497-500, 2007.
15. Lee, J.K., et al. *J. Am. Chem. Soc.* **130**, 3619-3623, 2008.
16. Thompson, B.C., et al. *J. Am. Chem. Soc.* **128**, 12714-12725, 2006.
17. Peet, J., et al. *Acc. Chem. Res.* **42** (11), 1700-1708, 2009.
18. Brabec, C.J., et al. *Adv. Funct. Mater.* **11** (1), 15-26, 2001.
19. Huynh, W.U., et al. *Adv. Funct. Mater.* **13** (1), 73-79, 2003.
20. Wu, M.C., et al. *J. Mater. Chem.* **18**, 4097-4102, 2008.
21. Peng, Z.A., & Peng, X. *J. Am. Chem. Soc.* **123**, 183-184, 2001.
22. Ravirajan, P., et al. *J. Phys. Chem. B* **110**, 7635-7639, 2006.
23. Beek, W.J.E., et al. *J. Phys. Chem. B* **109**, 9505-9516, 2005.
24. Könenkamp, R., et al. *Nano Lett.* **5** (10), 2005-2008, 2005.
25. Harnack, O., et al. *Nano Lett.* **3** (8), 1097-1101, 2003.
26. Kind, H., et al. *Adv. Mater.* **14** (2), 158-160, 2002.

27. Liu, B., & Zeng, H.C. *J. Am. Chem. Soc.* **125**, 4430-4431, 2003.
28. Jiang, Z.Y., et al. *J. Phys. Chem. B* **109**, 23269-23273, 2005.
29. Olson, D.C., et al. *J. Phys. Chem. C* **111**, 16670-16678, 2007.
30. Olson, D.C., et al. *Thin Solid Films* **496**, 26-29, 2006.
31. Bouclé, J., et al. *J. Phys. Chem. C* **114**, 3664-3674, 2010.
32. Beek, W.J.E., et al. *Adv. Mater.* **16** (12), 1009-1013, 2004.
33. Beek, W.J.E., et al. *J. Mater. Chem.* **15**, 2985-2988, 2005.
34. Coakley, K.M., & McGehee, M.D. *Appl. Phys. Lett.* **83**, 3380-3382, 2003.
35. Ravirajan, P., et al. *Adv. Funct. Mater.* **15** (4), 609-618, 2005.
36. Koster, L.J.A., et al. *Adv. Funct. Mater.* **17**, 1297-1302, 2007.
37. Das, N.C., et al. *J. Renew. Sust. Energ.* **3**, 033105, 2011, http://dx.doi.org/10.1063/1.3599838
38. Lee, T.H., et al. *Nanotechnology* **22**, 285401(1-6), 2011.
39. Moet, D.J.D., et al. *Chem. Mater.* **19**, 5856-5861, 2007.
40. Oosterhout, S.D., et al. *Nat. Mater.* **8**, 818-824, 2009.
41. Peiró, A.M., et al. *J. Mater. Chem.* **16**, 2088-2096, 2006.
42. Beek, W.J.E., et al. *Adv. Funct. Mater.* **16**, 1112-1116, 2006.
43. Oosterhout, S.D., et al. *Adv. Energy Mater.* **1**, 90-96, 2011.
44. Krebs, F.C. *Sol. Energ. Mater. Sol. Cells* **92**, 715-726, 2008.
45. Shrotriya, V., et al. *Appl. Phys. Lett.* **88**, 064104(1-3), 2006.
46. Si, L., et al. *Recent Patents on Materials Science* **5**, 166-172, 2012.
47. Yang, M.D., et al. *Opt. Express* **16** (20), 15754-15758, 2008.
48. Zhang, J.Z., & Noguez, C. *Plasmonics* **3**, 127-150, 2008.
49. Sau, T.K., et al. *Adv. Mater.* **22**, 1805-1825, 2010.
50. Stuart, H.R., & Hall, D.G. *Appl. Phys. Lett.* **69**, 2327-2329, 1996.
51. Wang, C.C.D., et al. *J. Mater. Chem.* **22**, 1206-1211, 2012.
52. Kim, K., & Carroll, D.L. *Appl. Phys. Lett.* **87**, 203113(1-3), 2005.
53. Spyropoulos, G.D., et al. *Appl. Phys. Lett.* **100**, 213904(1-5), 2012.
54. Wang, D.H., et al. *Angew. Chem. Int. Ed.* **50**, 5519-5523, 2011.
55. Fung, D.D.S., et al. *J. Mater. Chem.* **21**, 16349-16356, 2011.
56. Chen, F.C., et al. *Appl. Phys. Lett.* **95**, 013305(1-3), 2009.
57. Hsiao, Y.S., et al. *J. Phys. Chem. C* **116**, 20731-20737, 2012.
58. Spyropoulos, G.D., et al. *Photonic. Nanostruct.* **9**, 184-189, 2011.

59. Lee, J.H., et al. *Org. Electron.* **10**, 416-420, 2009.
60. Oo, T.Z., et al. *J. Phys. Chem. C* **116**, 6453-6458, 2012.
61. Schilinsky, P., et al. *Appl. Phys. Lett.* **81**, 3885-3887, 2002.
62. Padinger, F., et al. *Adv. Funct. Mater.* **13** (1), 85-88, 2003.
63. Roncali, J. *Macromol. Rapid Commun.* **28**, 1761-1775, 2007.
64. Ma, W., et al. *Adv. Funct. Mater.* **15**, 1617-1622, 2005.
65. Zhao, G., et al. *Adv. Mater.* **22**, 4355-4358, 2010.
66. Zhou, H., et al. *Macromolecules* **43**, 811-820, 2010.
67. Guo, X., et al. *Energy Environ. Sci.* **5**, 7943-7949, 2012.
68. Koizhaiganova, R.B., et al. *Synt. Met.* **159**, 2437-2442, 2009.
69. Mühlbacher, D., et al. *Adv. Mater.* **18**, 2884-2889, 2006.
70. Lenes, M., et al. *Adv. Mater.* **20**, 2116-2119, 2008.
71. Cozzens, R.F. Electrical Properties of Polymer, D.A. Seanor, Ed., Academic Press, New York, 1982, 93 (Chapter 3).
72. Wang, G., et al. *Physica B* **279**, 116-119, 2000.
73. Dridi, C., et al. *Nanotechnology* **19**, 375201(1-11), 2008.
74. Kaune, G., et al. *Eur. Phys. J. E* **26**, 73-79, 2008.
75. YanLing, J., et al. *Chin. Sci. Bull.* **53** (1), 46-52, 2008.
76. Pokhrel, B., et al. *Mater. Manuf. Process.* **27**, 43-48, 2012.
77. Yun, S., et al. *Prog. Polym. Sci.*; doi:10.1016/j.progpolymsci.2015.10.004
78. Nazeeruddin, Md.K., et al. *Sol. Energy* **85**, 1172-1178, 2011.
79. O'Regan, B., & Grätzel, M. *Nature* **353**, 737-740, 1991.
80. Su'ait, M.S., et al. *Int. J. Hydrogen energy* **39**, 3005-3017, 2014.
81. Akhtar, M.S., et al. *Electrochim. Acta* **55**, 2418-2423, 2010.
82. Fenton, D.E. *Polymer* **14** (11), 589, 1973.
83. Kubo, W., et al. *J. Phys. Chem. B* **105**, 12809-12815, 2001.
84. Kim, K.M., et al. *Bull. Korean Chem. Soc.* **27** (2), 322-324, 2006.
85. Benedetti, J.E., et al. *J. Power Sources* **208**, 263-270, 2012.
86. Kim, J.H., et al. *Chem. Commun.* 1662-1663, 2004.
87. Keis, K., et al. *Sol. Energ. Mater. Sol. Cells* **73**, 51-58, 2002.
88. Nahm, C., et al. *Appl. Phys. Lett.* **99**, 253107(1-4), 2011.
89. Cao, F., et al. *J. Phys. Chem.* **99**, 17071-17073, 1995.
90. Buraidah, M.H., et al. *Int. J. Photoenergy* 1-7, 2010; doi:10.1155/2010/805836

91. Lee, H.S., et al. *Curr. Appl. Phys.* **11**, S158-S162, 2011.
92. Lan, Z., et al. *J. Power Sources* **164**, 921-925, 2007.
93. Priya, A.R.S., et al. *Langmuir* **24**, 9816-9819, 2008.
94. Croce F., et al. *Nature* **394**, 456-458, 1998.
95. Khongchareon, N., et al. *Electrochim. Acta* **106**, 195-200, 2013.
96. Wang, Y.C., et al. *J. Mater. Chem.* **22**, 6982-6989, 2012.
97. Chang, Y.H., et al. *J. Mater. Chem.* **22**, 15592-15598, 2012.
98. Caseri, W. *Chem. Eng. Comm.* **196**, 549-572, 2009.
99. Dhas, V., et al. *Appl. Phys. Lett.* 93, 243108(1-3), 2008.
100. Brown, M.D., et al. *Nano Lett.* **11**, 438-445, 2011.
101. Xu, Q., et al. *Opt. Express* **20** (S6), A898-A907, 2012.
102. Akhtar, M.S., et al. *Electrochem. Commun.* **9**, 2833-2837, 2007.
103. Morales, P.V., et al. *Electrochim. Acta* **43** (10-11), 1275-1279, 1998.
104. Huang, X., et al. *Electrochim. Acta* **80**, 219-226, 2012.
105. Rani, M.S.A., et al. *Polymers* **6**, 2371-2385, 2014.
106. Bella, F., et al. *Chem. Eng. Trans.* **41**, 211-216, 2014.
107. Singh, R., et al. *Int. J. Electrochem. Sci.* **9**, 2620-2630, 2014.
108. Singh, R., et al. *Carbohyd. Polym.* **91**, 682-685, 2013.
109. Yusuf, S.N.F., et al. *J. Chem.* 1-8, 2014.
110. Vieira, D.F., et al. *Electrochim. Acta* **53**, 1404-1408, 2007.
111. Choudhury, N.A., et al. *J. Electrochem. Soc.* **155** (1), A74-A81, 2008.
112. Wieczorek, W., et al. *J. Phys. Chem.* **98**, 9047-9055, 1994.
113. Siekierski, M., et al. *Electrochim. Acta* **43** (10-11), 1339-1342, 1998.
114. Wieczorek, W., et al. *J. Phys. Chem. B* **102**, 352-360, 1998.
115. Golodnitsky, D., et al. *Solid State Ionic.* **85**, 231-238, 1996.
116. Silva, M.M., et al. *Opt. Mater.* **32**, 719-722, 2010.
117. Kahlout, A.A., et al. *Ionics* **16**, 13-19, 2010.
118. Alves, R.D., et al. *Electroanal.* **25** (6), 1483-1490, 2013.
119. Leones, R., et al. *Opt. Mater.* **35**, 187-195, 2012.
120. Vieira, D.F., & Pawlicka, A. *Electrochim. Acta* **55**, 1489-1494, 2010.
121. Bauer, W., & Heiland, G. *J. Phys. Chem. Solids* **32**, 2605-2611, 1971.
122. Keis, K., et al. *Nanostruct. Mater.* **12**, 487-490, 1999.
123. Rensmo, H., et al. *J. Phys. Chem. B* **101**, 2598-2601, 1997.

124. Redmond, G., et al. *Chem. Mater.* **6**, 686-691, 1994.
125. Solbrand, A., et al. *Sol. Energ. Mat. Sol. Cells* **60**, 181-193, 2000.
126. Quintana, M., et al. *J. Phys. Chem. C* **111**, 1035-1041, 2007.
127. Keis, K., et al. *J. Photochem. Photobiol. A: Chem.* **148**, 57-64, 2002.
128. O'Regan, B., et al. *Adv. Mater.* **12** (17), 1263-1267, 2000.
129. Boucharef, M., et al. *Nanotechnology* **21**, 205203(1-12), 2010.
130. Nelson, J., & Chandler, R.E. *Coordin. Chem. Rev.* **248**, 1181-1194, 2004.
131. Feng, X., et al. *Nano Lett.* **8** (11), 3781-3786, 2008.
132. Liu, B., & Aydil, E.S. *J. Am. Chem. Soc.* **131**, 3985-3990, 2009.
133. Baxter, J.B., & Aydil, E.S. *Appl. Phys. Lett.* **86**, 053114(1-3), 2005.
134. Zhang, Q., & Cao, G. *Nano Today* **6**, 91-109, 2011
135. Han, J., et al. *Nanotechnology* **21**, 405203(1-7), 2010.
136. Martinson, A.B.F., et al. *Nano Lett.* **7** (8), 2183-2187, 2007.
137. Martinson, A.B.F., et al. *J. Phys. Chem. A* **113**, 4015-4021, 2009.
138. Martinson, A.B.F., et al. *Chem. Eur. J.* **14**, 4458-4467, 2008.
139. Gan, X., et al. *Thin Solid Films* **518**, 4809-4812, 2010.
140. Sacco, A., et al. *Phys. Chem. Chem. Phys.* **14**, 16203-16208, 2012.
141. Ku, C.H., & Wu, J.J. *Nanotechnology* **18**, 505706(1-9), 2007.
142. Yodyingyong, S., et al. *Appl. Phys. Lett.* **96**, 073115(1-3), 2010.
143. Kim, I.D., et al. *Appl. Phys. Lett.* **91**, 163109(1-3), 2007.
144. Ku, C.H., & Wu, J. *J. Appl. Phys. Lett.* **91**, 093117(1-3), 2007.
145. Zhang, H., et al. *Mater. Chem. Phys.* **93**, 65-69, 2005.
146. Jiu, J., et al. *J. Phys. Chem. B* **110**, 2087-2092, 2006.
147. Baruah, S., & Dutta, J. *J. Sol-Gel Sci. Technol.* **50**, 456-464, 2009.
148. Li, Z., et al. *Inorg. Chem.* **42**, 8105-8109, 2003.
149. Vayssieres, L., et al. *J. Phys. Chem. B* **105**, 3350-3352, 2001.
150. Zhai, H.J., et al. *Mater. Chem. Phys.* **112**, 1024-1028, 2008.
151. Shinde, S.D., et al. *Int. J. smart sensing intell. syst.* **5** (1), 57-70, 2012.
152. Murphy, C.J., et al. *Inorg. Chem.* **45**, 7544-7554, 2006.
153. Gao, J., et al. *Langmuir* **19**, 9065-9070, 2003.
154. Niu, W., & Xu, G. *Nano Today* **6**, 265-285, 2011.
155. Tao, A., et al. *Angew. Chem. Int. Ed.* **45**, 4597-4601, 2006.
156. Jana, N.R., et al. *J. Phys. Chem. B* **105**, 4065-4067, 2001.

157. Gole, A., & Murphy, C.J. *Chem. Mater.* **16**, 3633-3640, 2004.
158. Nikoobakht, B., & El-Sayed, M.A. *Chem. Mater.* **15**, 1957-1962, 2003.
159. Penwell, R.C., et al. *J. Polym. Sci. Macromol. Rev.* **13**, 63-160, 1978.
160. Jones, R.G., et al. *J.C.S. Chem. Comm.* 22-23, 1972.
161. Boddula, R., & Srinivasan, P. *International Scholarly Research Notices*, 1-8, 2014.
162. Kamogawa, H., et al. *J. Polym. Sci. Polym. Chem. Ed.* **18**, 9-18, 1979.
163. Han, Z., et al. *Sol. Energ. Mat. Sol. Cells* **95**, 483-490, 2011.
164. Amou, S., et al. *J. Polym. Sci. Polym. Chem.* **37**, 1943-1948, 1999.
165. Hotta, S., et al. *Synth. Met.* **26** (3), 267-279, 1988.
166. Niemi, V.M., et al. *Polymer* **33**, 1559-1562, 1992.
167. Kulszewicz-Bajer, I., et al. *Synth. met.* **30** (3), 335-339, 1989.
168. Leclerc, M., et al. *Makromol. Chem.* **190**, 3105-3116, 1989.
169. Zu, Y., et al. *Int. J. Biol. Macromolec.* **50**, 82-87, 2012.
170. Tabata, Y., & Ikada, Y. *Pharm. Res.* **6**, 422-427, 1989.
171. Yamamoto, M., et al. *J. Control. Rel.* **64**, 133-142, 2000.
172. Nimni, M.E., et al. *J. Biomed. Mater. Res.* **21**, 741-771, 1987.
173. Gorman, S.P., et al. *J. Appl. Bacteriol.* **48**, 161-190, 1980.
174. Nomori, H., et al. *Ann. Thorac. Surg.* **67**, 212-216, 1999.
175. Konishi, M., et al. *J. Control. Release* **92**, 301-313, 2003.
176. Draye, J.P., et al. *Biomaterials* **19**, 1677-1687, 1998.
177. Mattos, R.I., et al. *Mol. Cryst. Liq. Cryst.* **483**, 120-129, 2008.
178. Sanchez, C., et al. *Chem. Soc. Rev.* **40**, 471-472, 2011.
179. Sanchez, C., et al. *Nat. Mater.* **4**, 277-288, 2005.
180. Sanchez, C., et al. *Chem. Soc. Rev.* **40**, 696-753, 2011.
181. Baker, C., et al. *J. Magn. Magn. Mater.* **280**, 412-418, 2004.
182. Shin, S., et al. *Catal. Commun.* **10**, 178-182, 2008.
183. Farah, A.A., et al. *J. Colloid Interface Sci.* **319**, 572-576, 2008.
184. Wang, T.L., et al. *Macromol. Rapid Commun.* **30**, 1679-1683, 2009.
185. Jang, E., et al. *Polym. Adv. Technol.* **21**, 476-482, 2010.